Updates from GWTC-4 and latest results from the search for an Isotropic GWB from LVK's O4a

Presented By

Dr. Alba Romero-Rodríguez

Seminaire LAPP Janvier 2026

23rd of January 2026

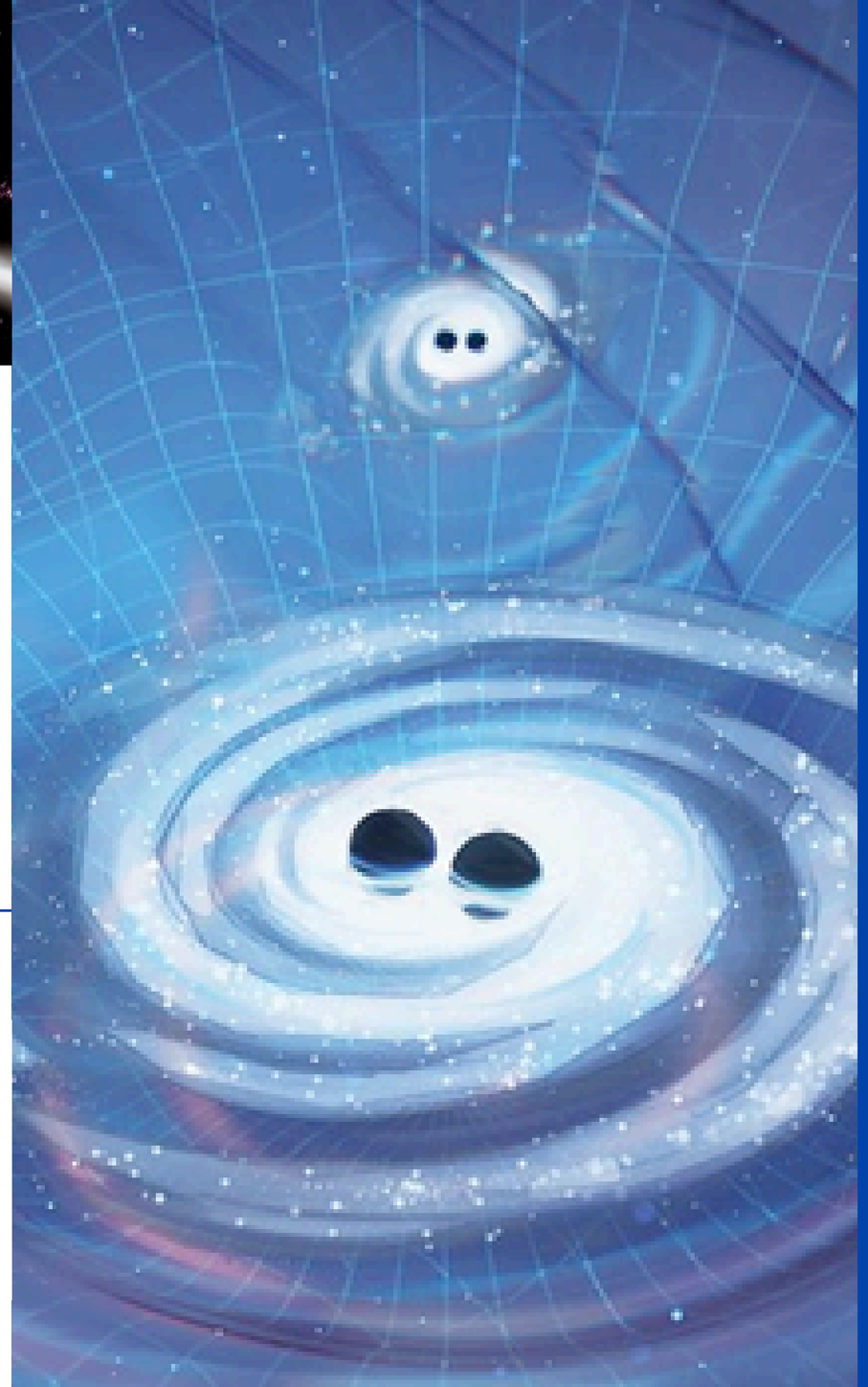

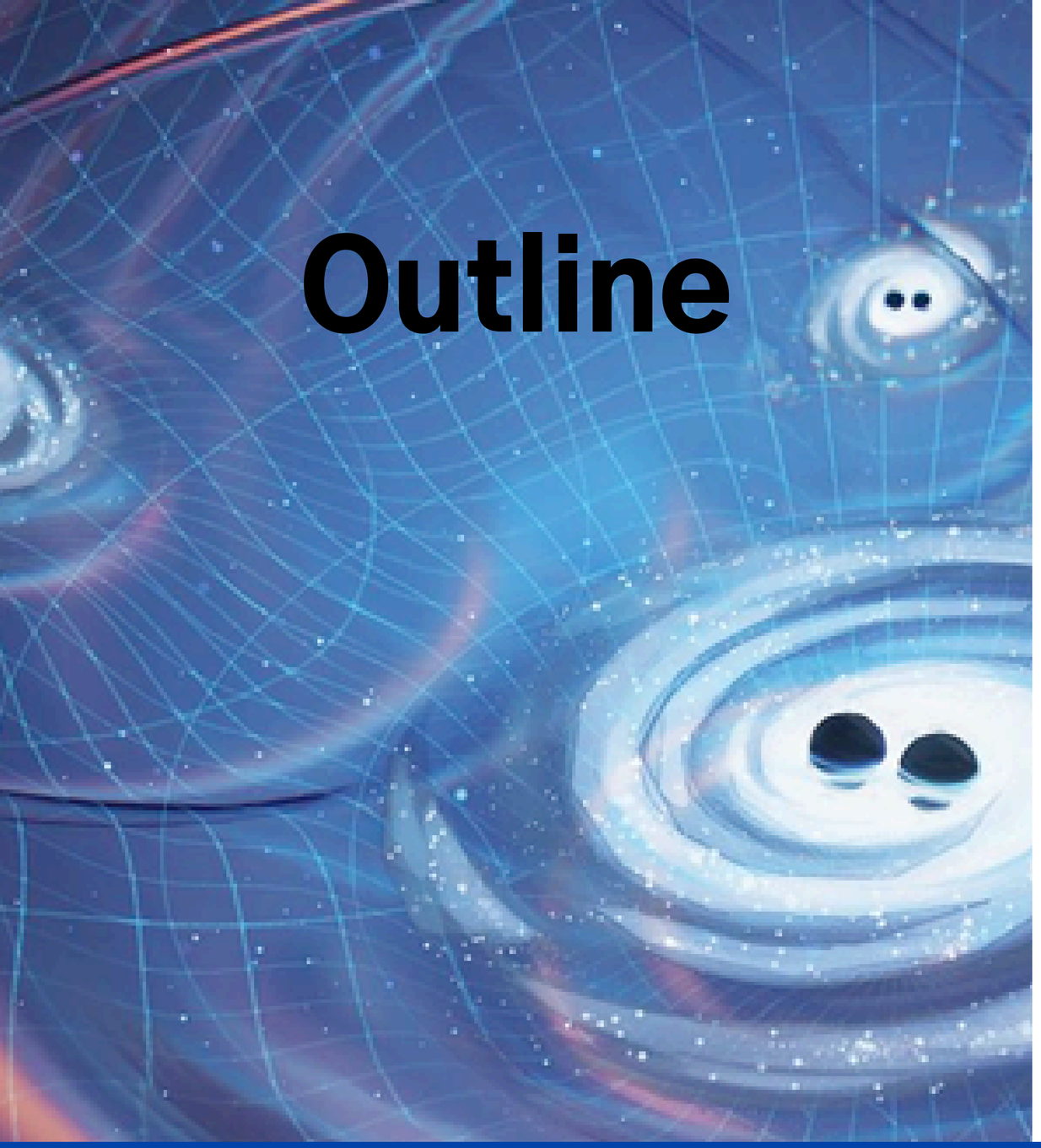

Outline

1 Introduction to gravitational waves (GWs)

2 Sources of GWs

3 Updates on GWTC-4

4 Gravitational wave background (GWB)

5 LVK search for an isotropic GWB

6 Latest LVK results on the search for an isotropic GWB

7 Conclusions

Introduction to GWs

- General relativity (GR) is the best available theory of gravity
- It describes the interaction between massive bodies as an effect of the curvature of spacetime
- In Einstein's universe, objects moving freely under the effects of gravity simply follow ***geodesic*** paths dictated by the ***curvature of spacetime.***

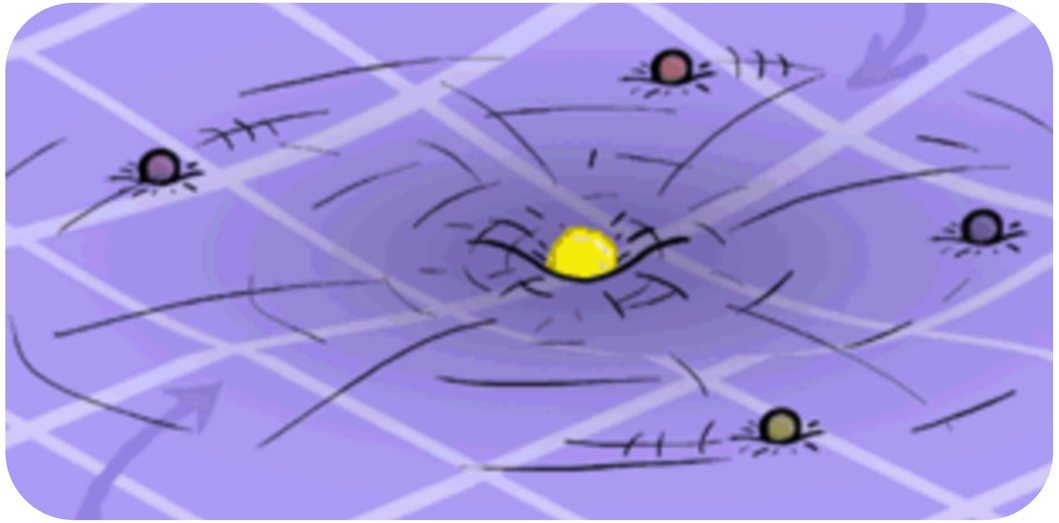

Introduction to GWs – Einstein equations

$$R_{\mu\nu} - \frac{1}{2} g_{\mu\nu} R = -\frac{8\pi G}{c^4} T_{\mu\nu}$$

Introduction to GWs – Einstein equations

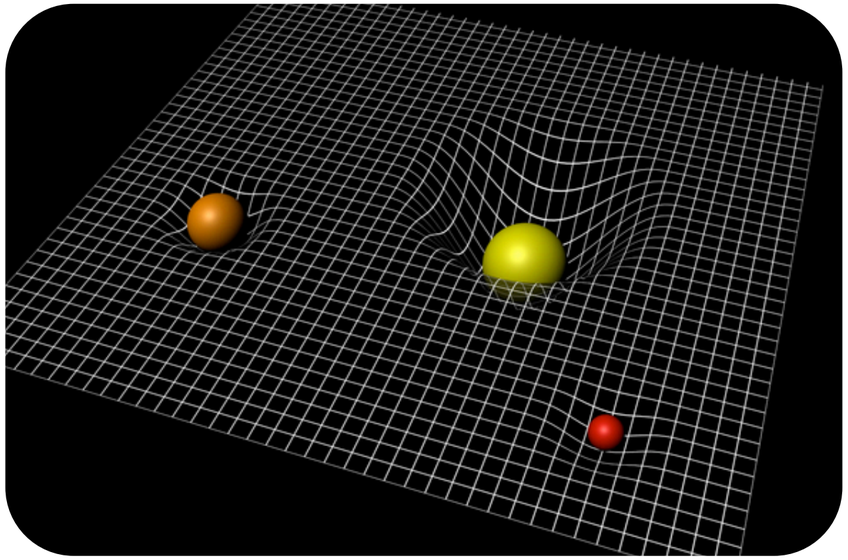

$$R_{\mu\nu} - \frac{1}{2} g_{\mu\nu} R = -\frac{8\pi G}{c^4} T_{\mu\nu}$$

Space-time curvature part

Mass/energy distribution part

Derivation Gravitational waves

- Weak field limit: Minkowski + perturbation

$$g_{\mu\nu} = \eta_{\mu\nu} + h_{\mu\nu} \qquad |h_{\mu\nu}| << 1$$

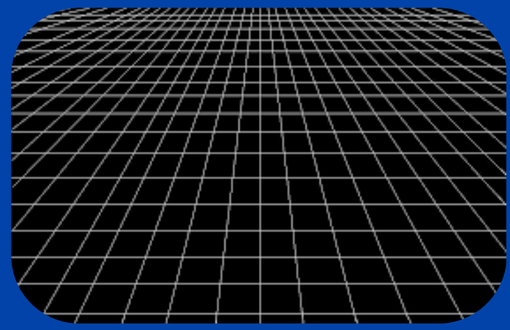

- We can simplify E. Eqs by assuming an appropriate gauge (Lorentz):

$$\Box \bar{h}_{\mu\nu} \equiv \partial^{\sigma}\partial_{\sigma}\bar{h}_{\mu\nu} = -\frac{16\pi G}{c^4}T_{\mu\nu}$$

- Far away from any source of mass/energy ($T_{\mu\nu} = 0$), E. eqs. are a 4D wave equation with sols.: **plane waves**

$$\bar{h}^{\mu\nu} = A^{\mu\nu}\, e^{ik_{\alpha}x^{\alpha}}$$

Derivation Gravitational waves

- These are the **GRAVITATIONAL WAVES (GW)!!**

$$\bar{h}^{\mu\nu} = A^{\mu\nu} e^{ik_\alpha x^\alpha}$$

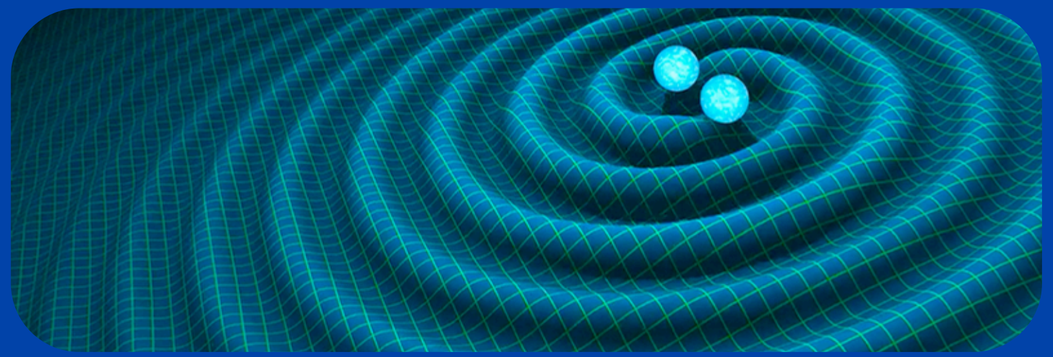

- Properties:
  - $\omega^2 = |k_i|^2$, $|k_i| = \omega/v \longrightarrow v = c = 1$

    GWs travel at the speed of light
  - Applying Lorentz gauge to E. eqs.: $k_\mu A^{\mu\nu} = 0$

    GWs are transverse

GW polarizations

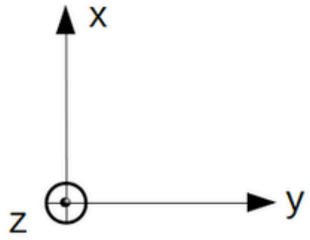

- Lorentz gauge + Transverse Traceless (TT) gauge: leave only 2 degrees of freedom in hμν

- For GWs propagating in the +z direction

$$h_{\mu\nu} = \begin{pmatrix} 0 & 0 & 0 & 0 \\ 0 & h_+ & h_x & 0 \\ 0 & h_x & -h_+ & 0 \\ 0 & 0 & 0 & 0 \end{pmatrix}$$

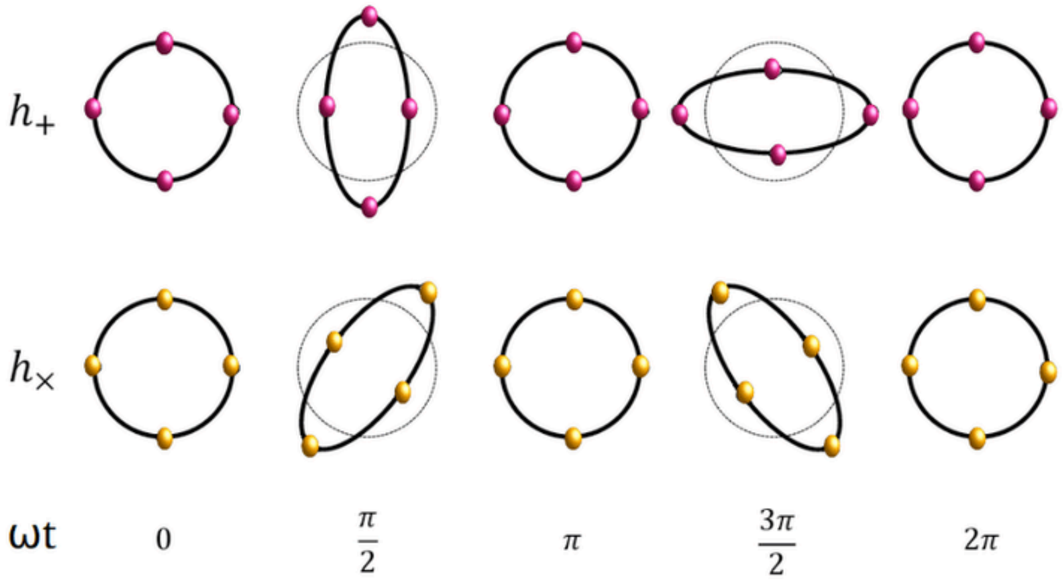

h+ is the plus polarization of the GW

$$h_+(t,z) \equiv A_+ \cos(\omega(t - z/c) + \phi_+)$$

$$h_x(t,z) \equiv A_x \cos(\omega(t - z/c) + \phi_x).$$

hx is the cross polarization of the GW

Generation of GWs

Any assymetrical body in rotation will generate GWs

Amplitude of GWs generated by Compact Binary Coalescences (CBCs) is measurable

Amplitude of GWs generated by light bodies is not measurable yet

GW emission, quadrupole formalism – example

- Objective: determine magnitude of the strain produced by a binary system of objects with masses m1 and m2 in a circular orbit with radius R

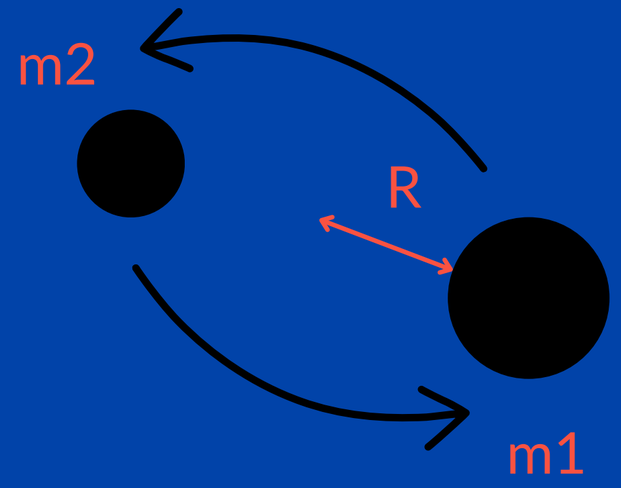

Assuming masses are m1 = m2 = 1kg, D = 10^3 km (distance from source to observer) and R = 1m → strain is: 5.9×10^{-35}

GW detection

- In our detectors, strain is defined as: $h = \Delta L / L$
  - ΔL: difference in length between the two arms
  - L: nominal length of an arm
- In Virgo (L = 3km), to detect $h = 5.9 \times 10^{-35}$ we would need to be sensitive to variations in length of: $\Delta L \sim 2 \times 10^{-31}$ m → unfeasible

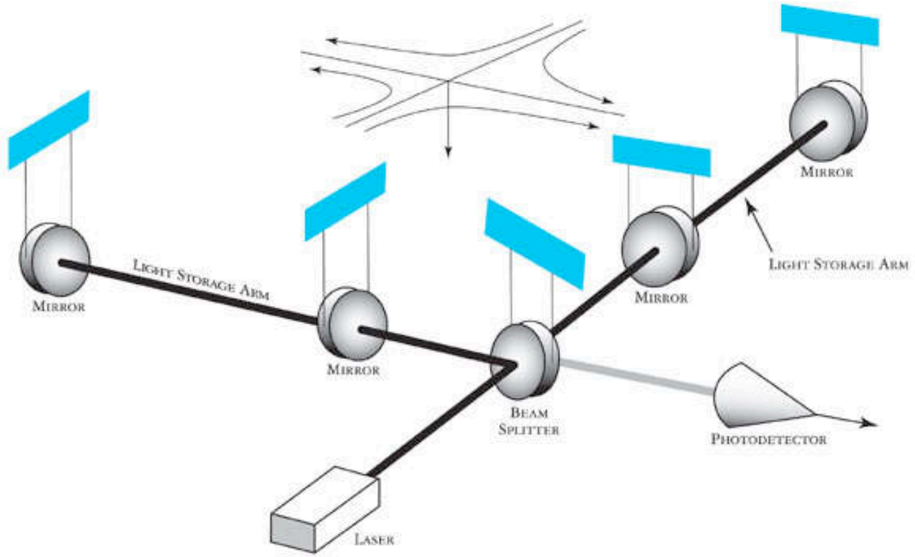

GW detection – LVK network

- International collaborations of ground based detectors:
  - LIGO
  - Virgo
  - KAGRA
- We just finished the fourth observing run (O4)

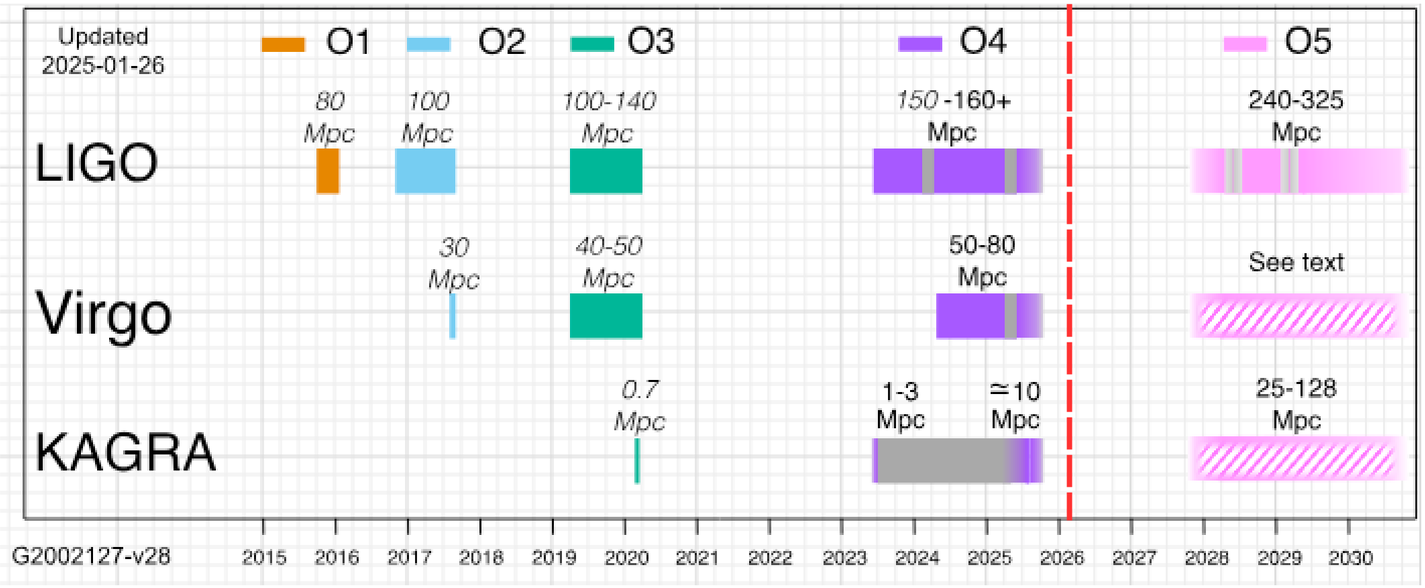

Sources of GWs

	Modelled	Unmodelled
Short duration		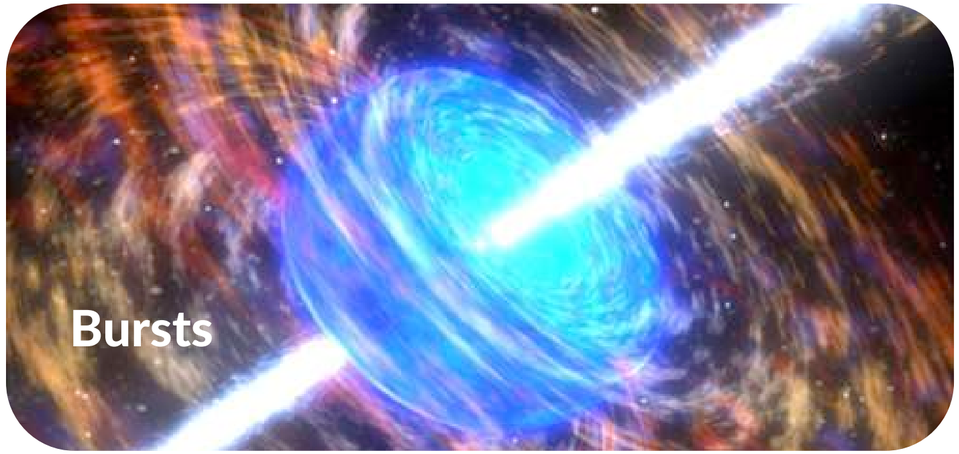
Long duration	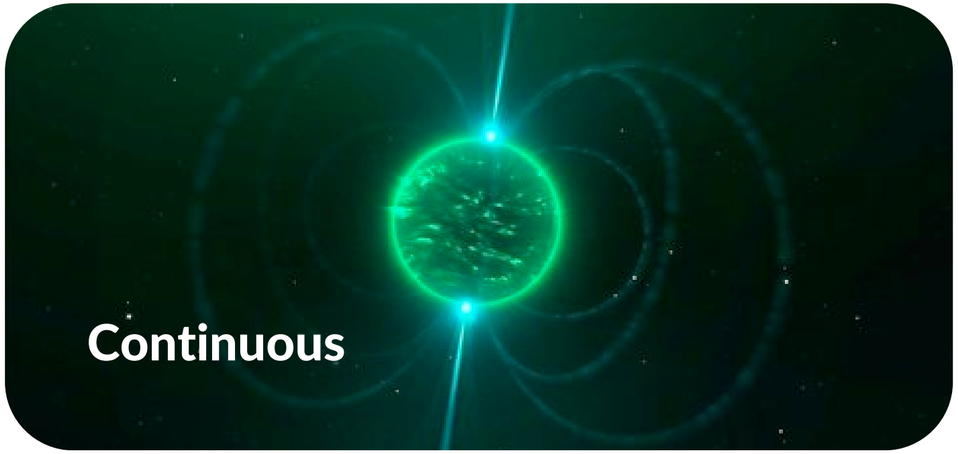	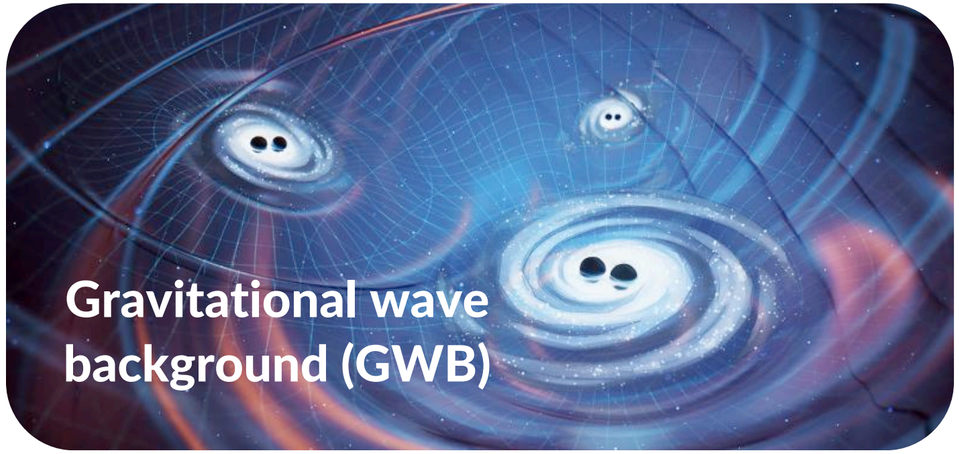

Sources of GWs

Modelled

Unmodelled

Short duration

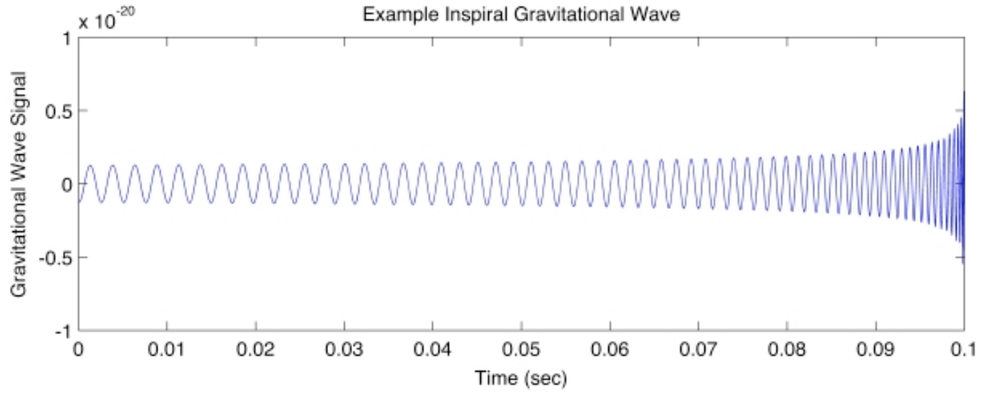

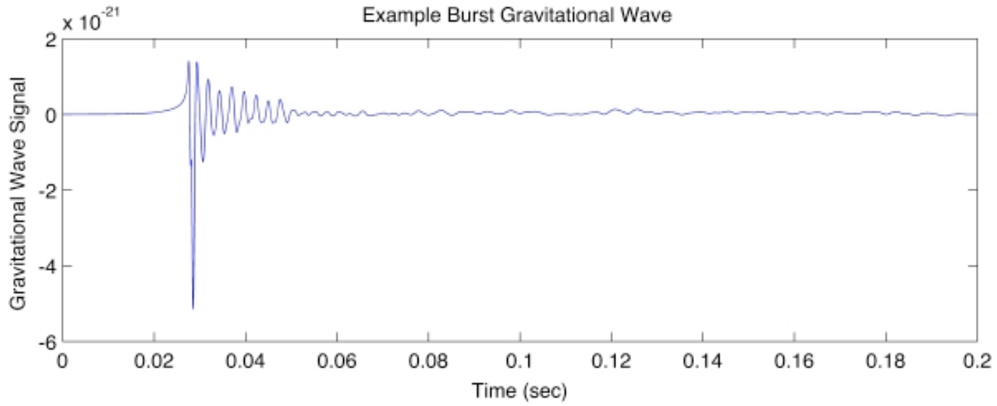

Long duration

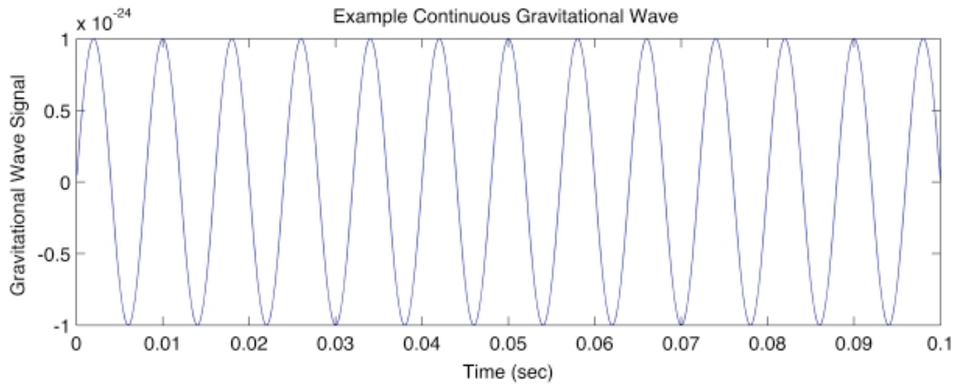

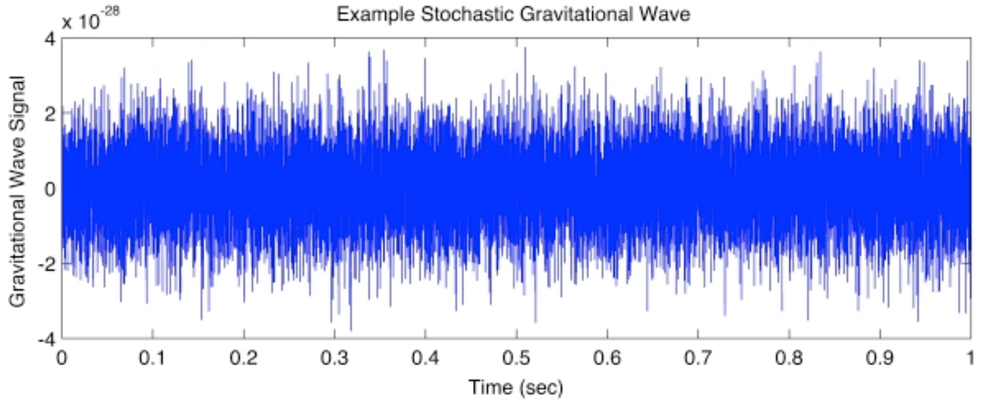

Sources of GWs

Modelled

Unmodelled

Short duration

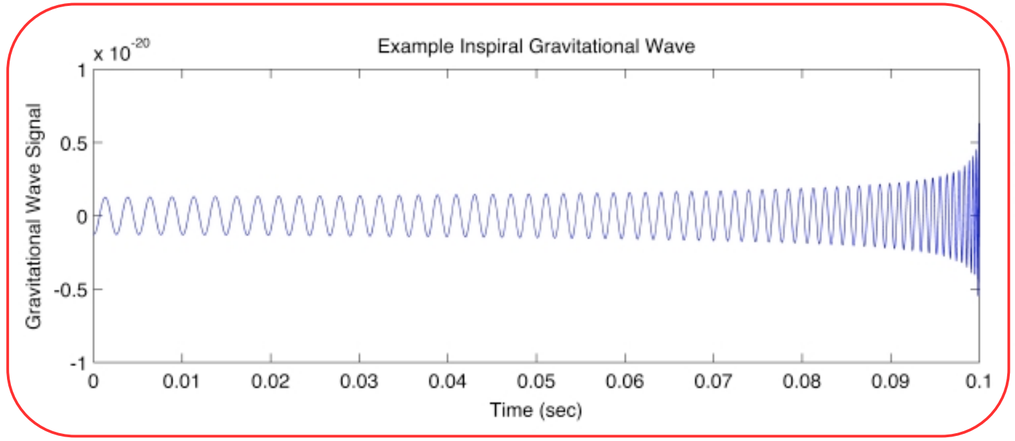

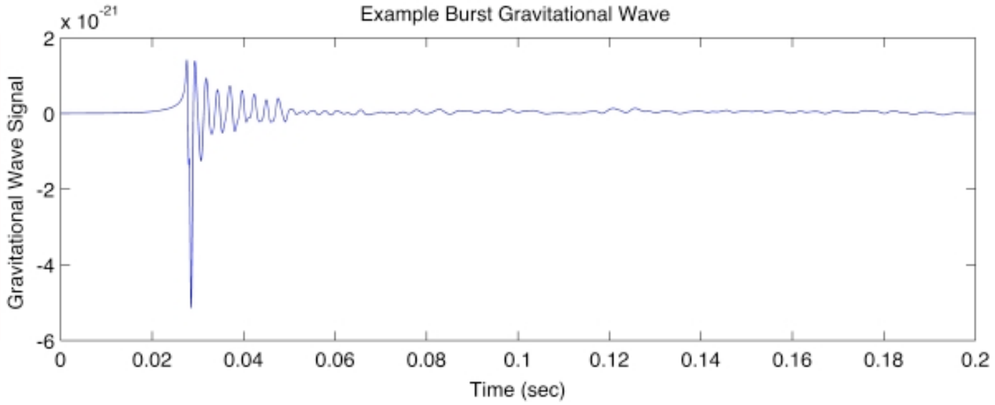

Long duration

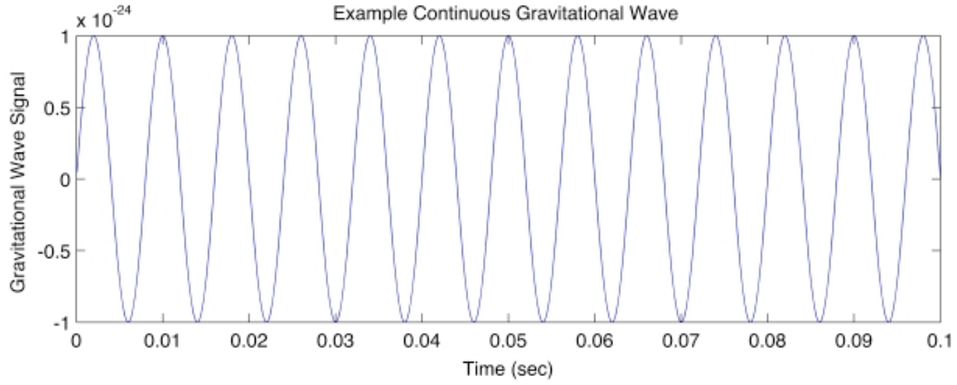

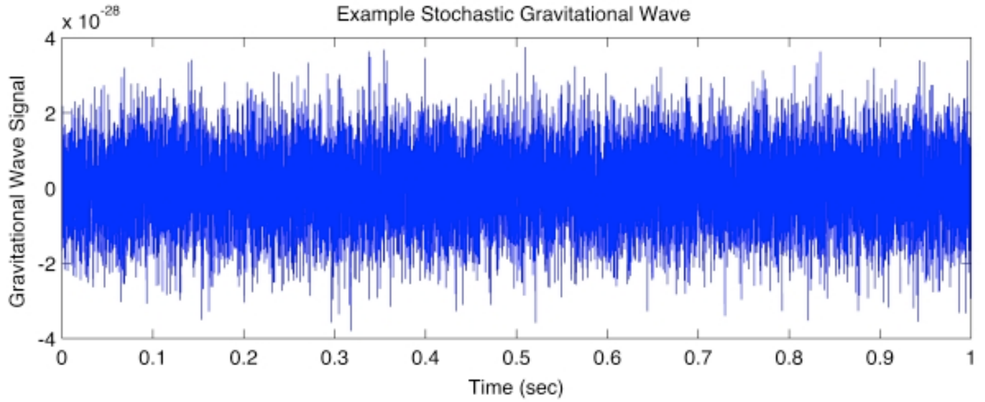

Sources of GWs

$$h = \frac{\Delta L}{L}$$

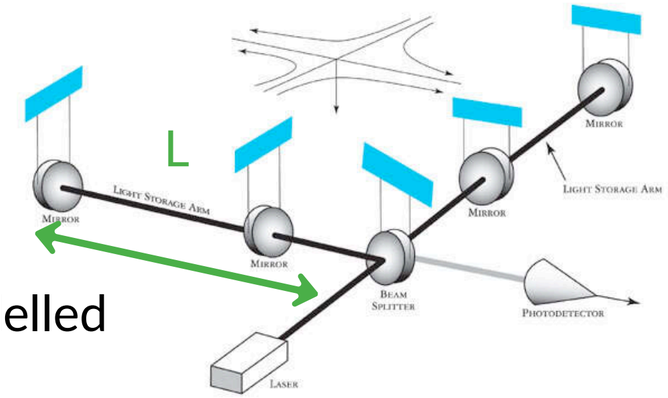

Modelled

Unmodelled

Short duration

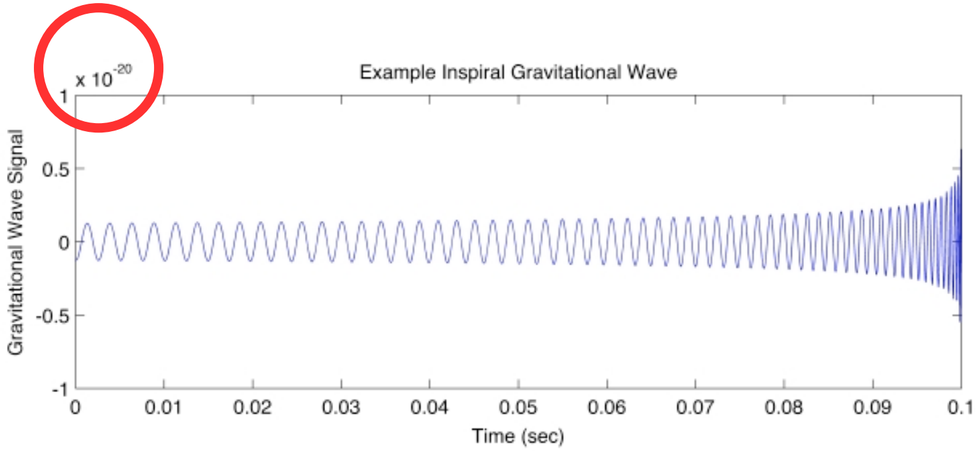

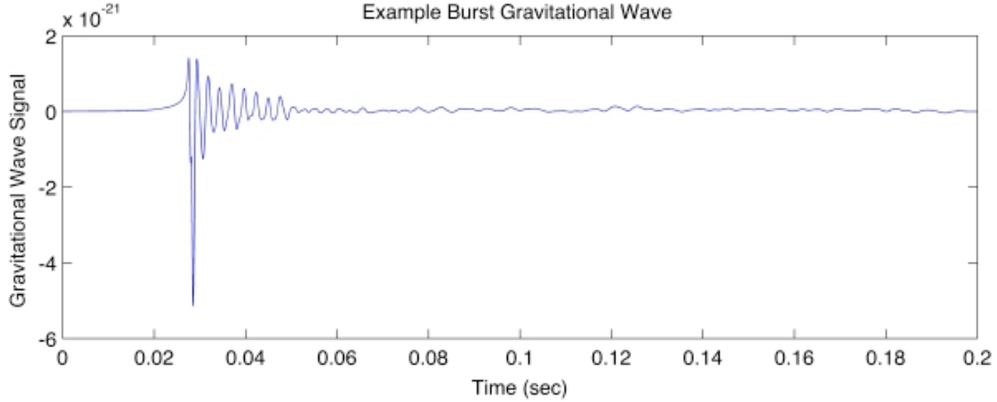

Long duration

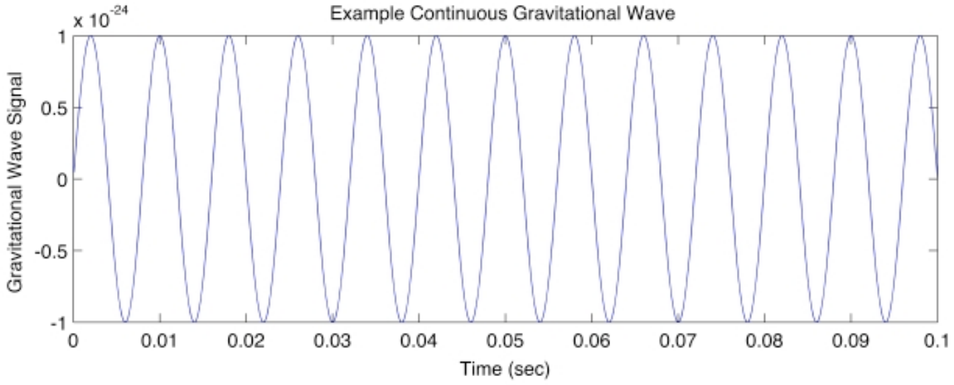

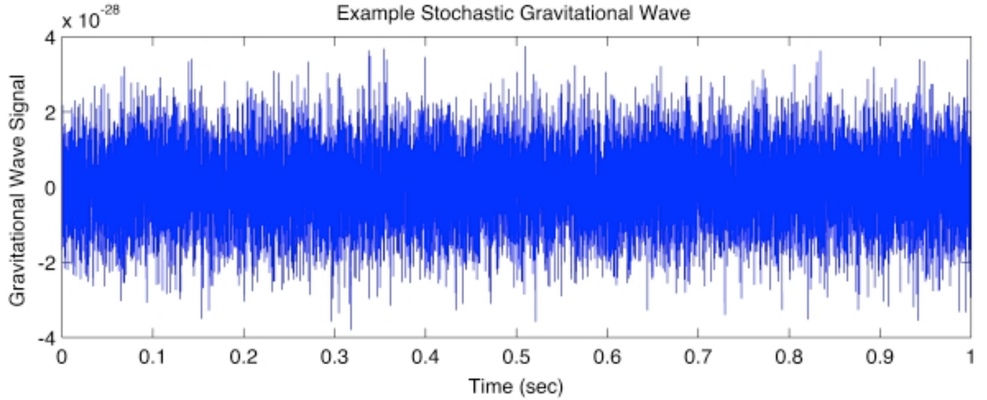

Sources of GWs

Modelled

Unmodelled

Short duration

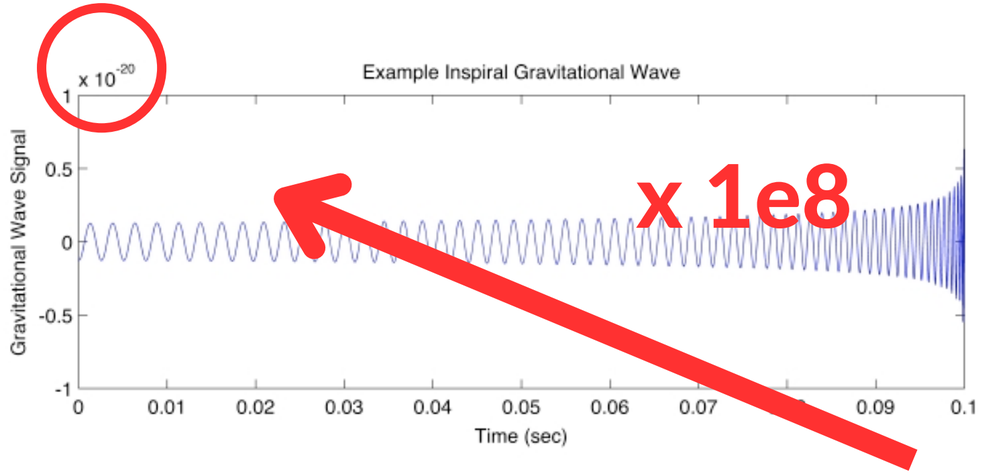

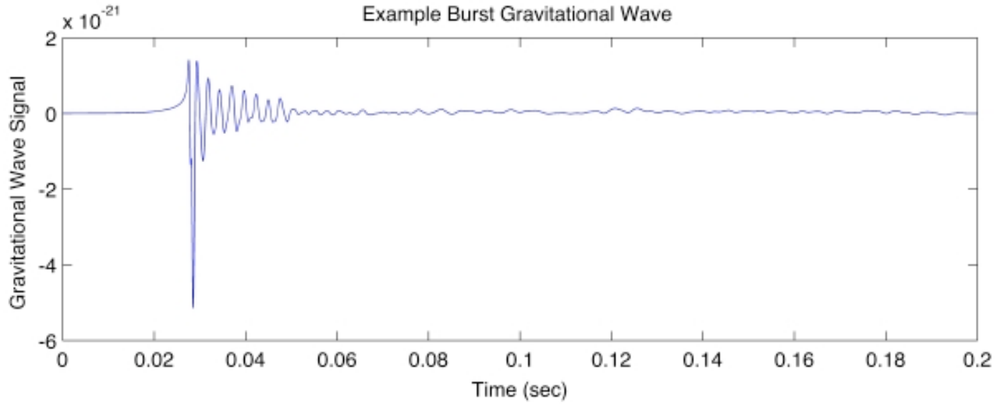

Long duration

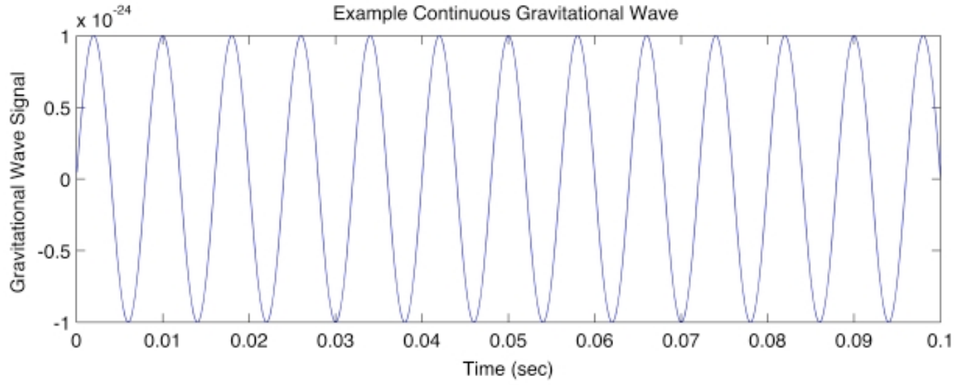

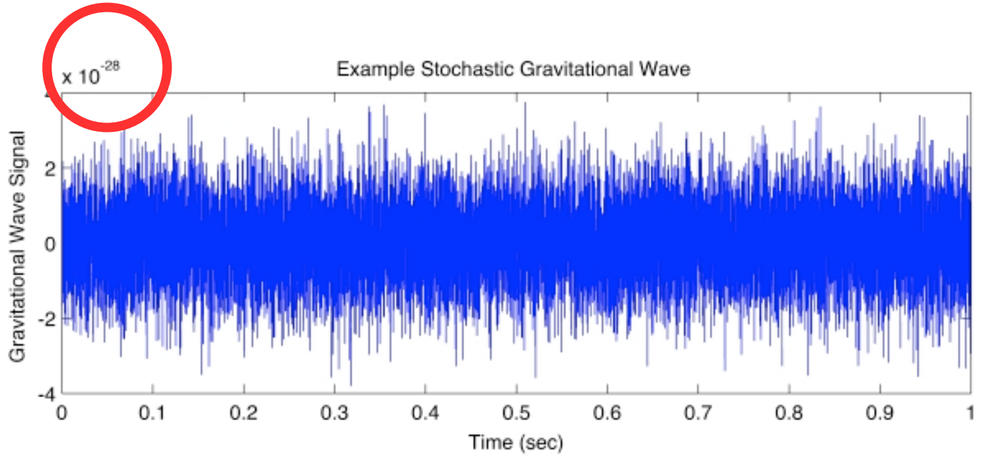

Sources of GWs

Modelled

Unmodelled

Short duration

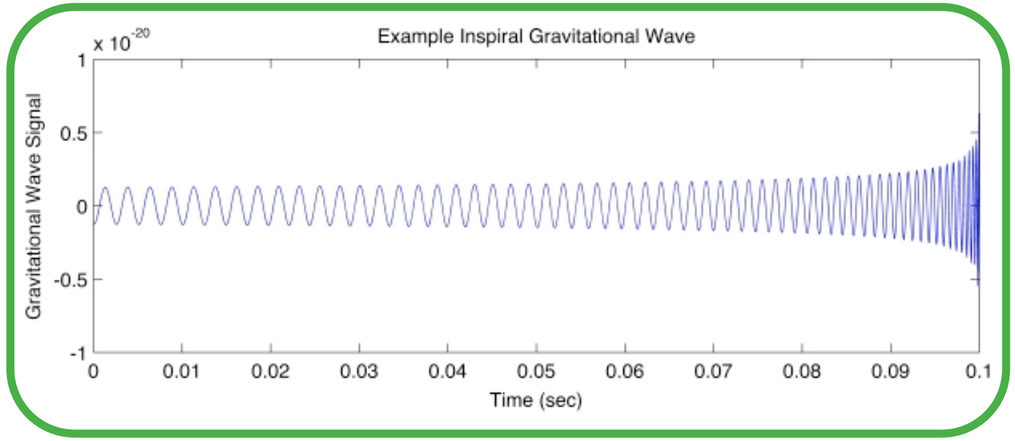

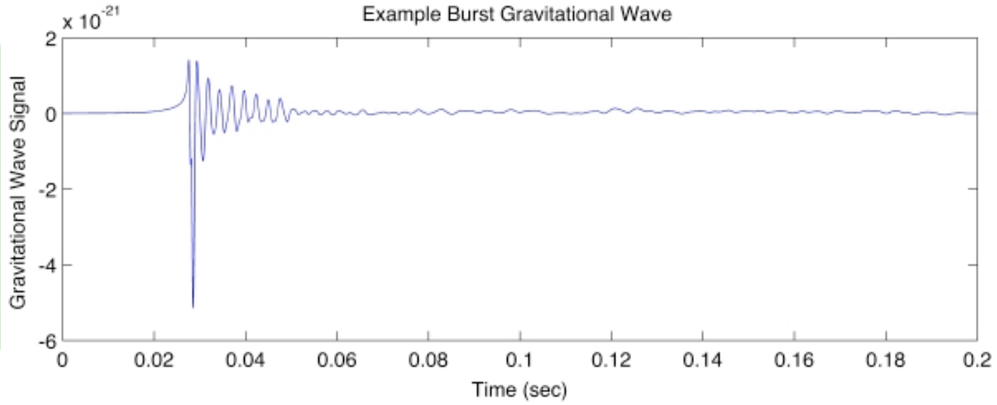

Long duration

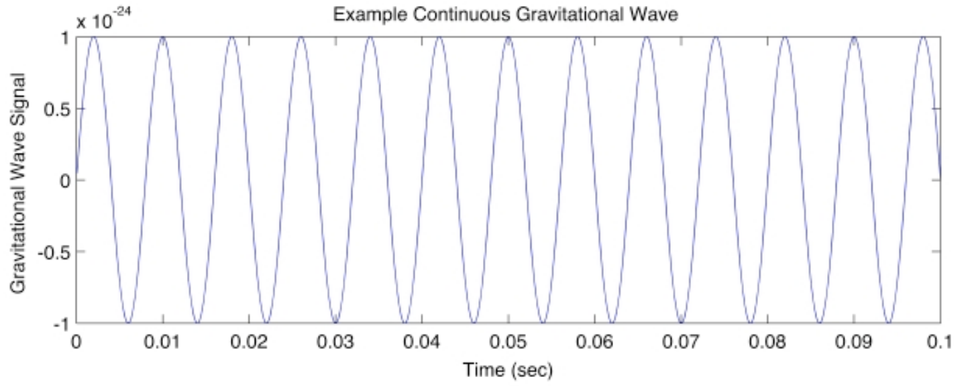

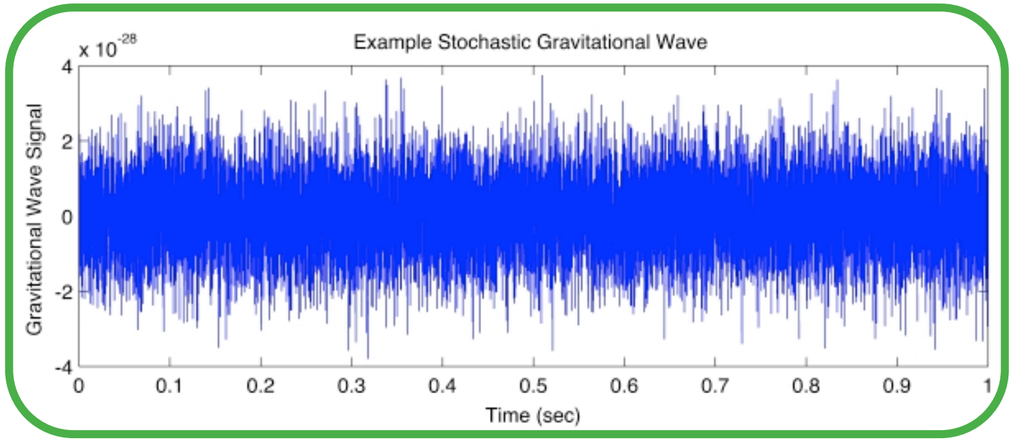

Updates from the fourth release of the Gravitational Wave Transient Catalog (GWTC-4)

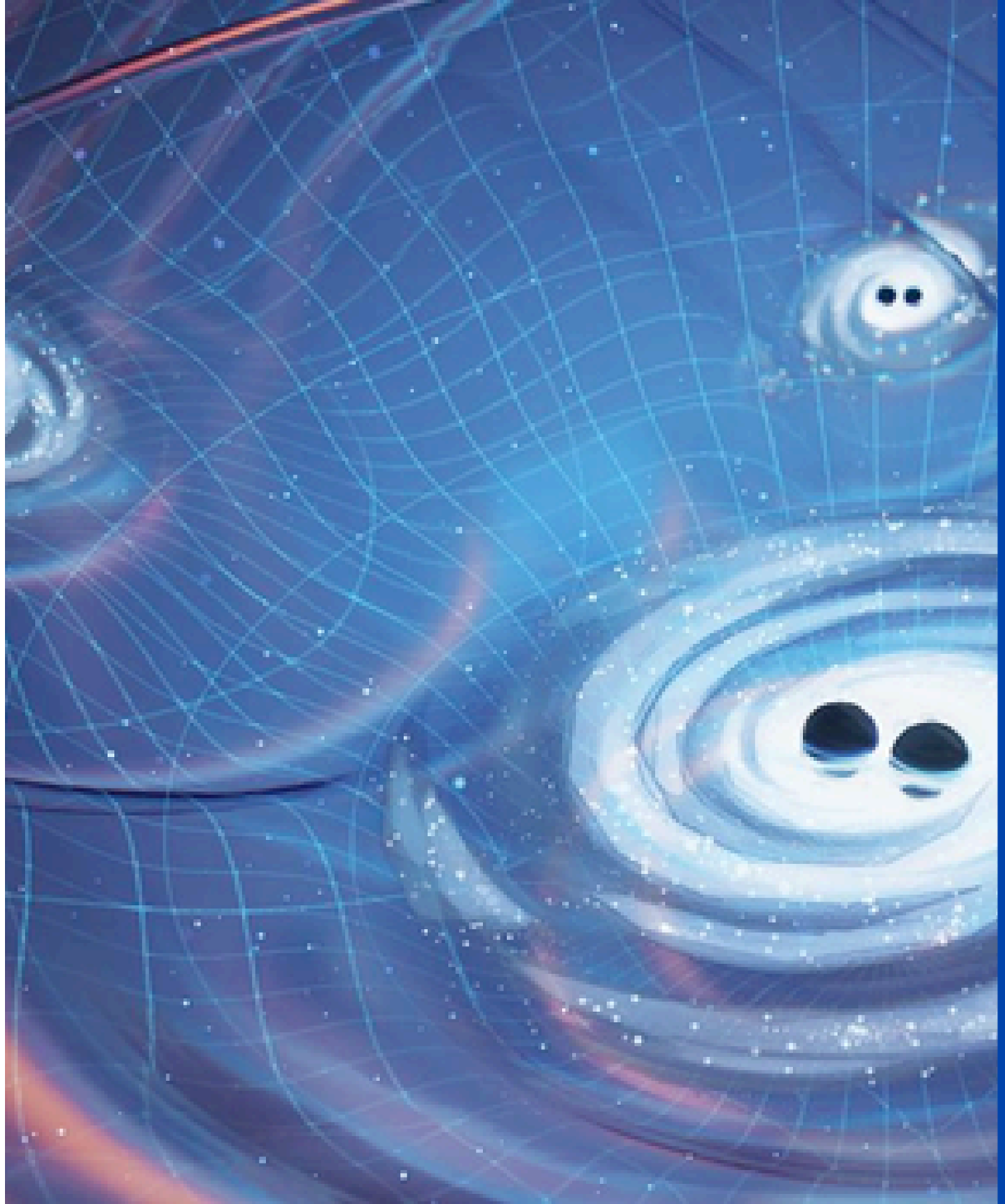

GWTC–4: Methods

- Search is carried out in 2 stages:
  - Online analyses → EM follow-up
  - Offline analyses → more accuracy
- Two types of detection algorithms:
  - Pipelines not relying on waveforms
  - Pipelines relying on waveforms: matched filtering

$$\rho(t) = 4 \left| \int_{f_{\text{low}}}^{f_{\text{high}}} \frac{h(f) u^*(f|\boldsymbol{\theta}_{\text{int}})}{S_n(f)} e^{2i\pi f t} df \right|$$

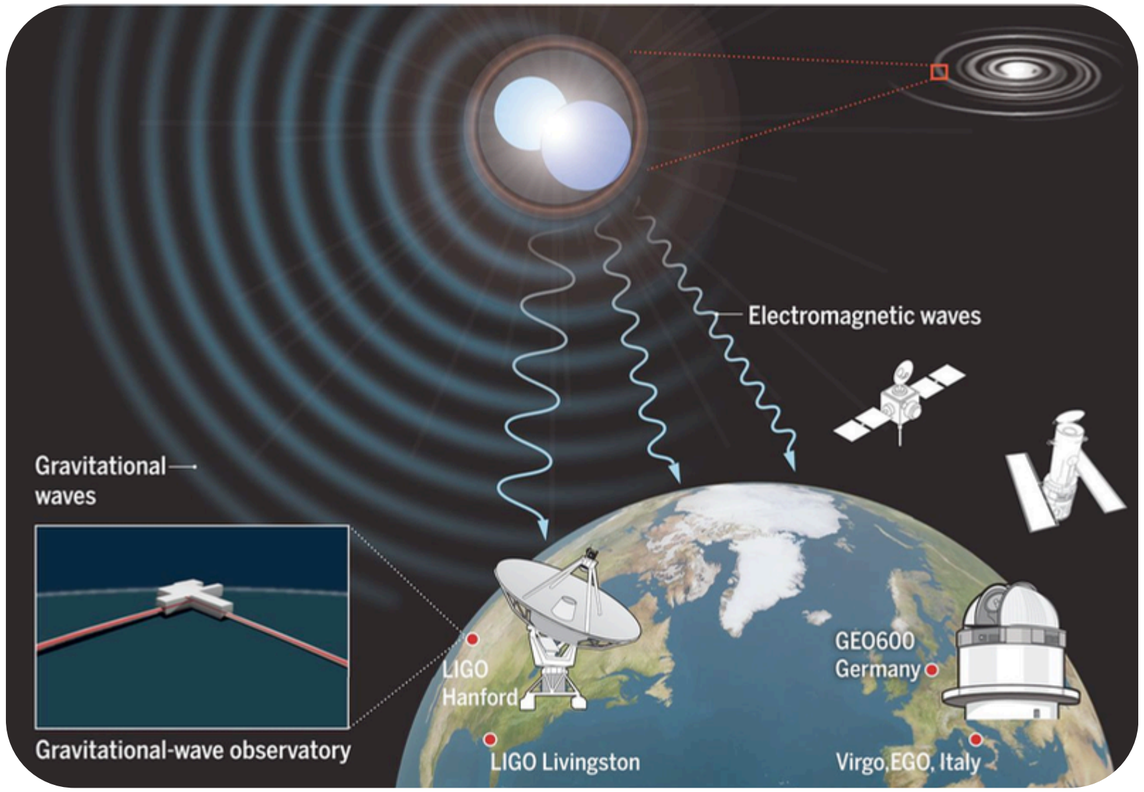

GWTC-4: Methods

- Search is carried out in 2 stages:
  - Online analyses → EM follow-up
  - Offline analyses → more accuracy
- Two types of detection algorithms:
  - Pipelines not relying on waveforms
  - Pipelines relying on waveforms: matched filtering

$$\rho(t) = 4 \left| \int_{f_{\rm low}}^{f_{\rm high}} \frac{h(f)\, u^*(f|\boldsymbol{\theta}_{\rm int})}{S_n(f)} e^{2i\pi f t} df \right|$$

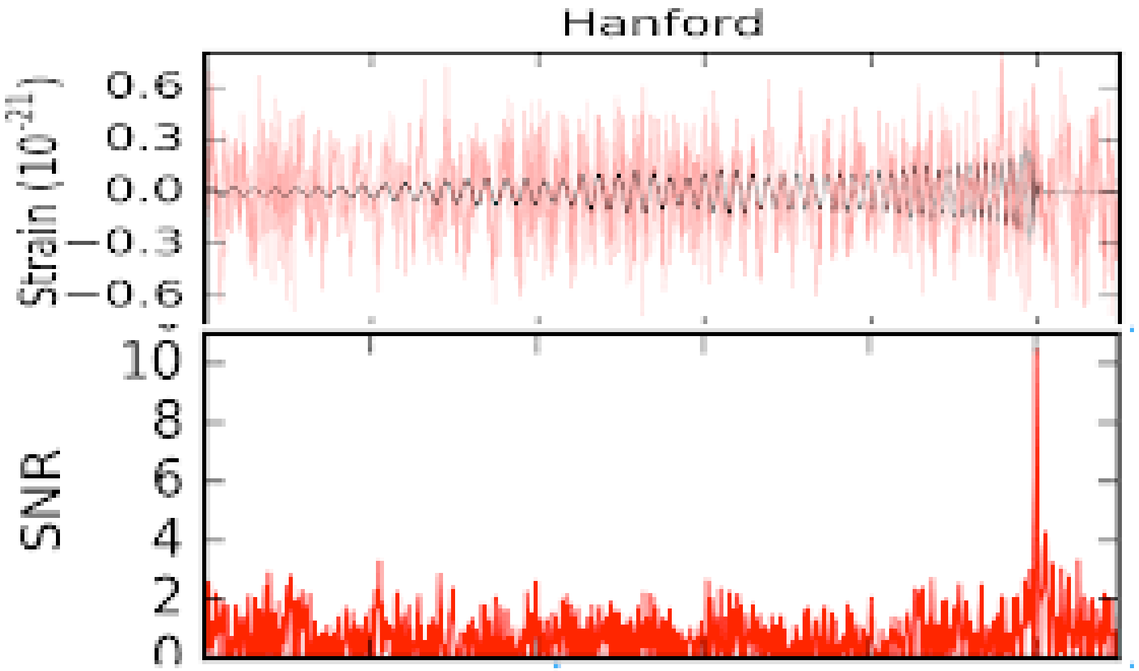

Strain data

GWTC-4: Methods

LVK Collaboration, arXiv:2508.18081 (2025)

- Search is carried out in 2 stages:
  - Online analyses → EM follow-up
  - Offline analyses → more accuracy
- Two types of detection algorithms:
  - Pipelines not relying on waveforms
  - Pipelines relying on waveforms: matched filtering

$$\rho(t) = 4 \left| \int_{f_{\text{low}}}^{f_{\text{high}}} \frac{h(f) u^*(f|\boldsymbol{\theta}_{\text{int}})}{S_n(f)} e^{2i\pi f t} df \right|$$

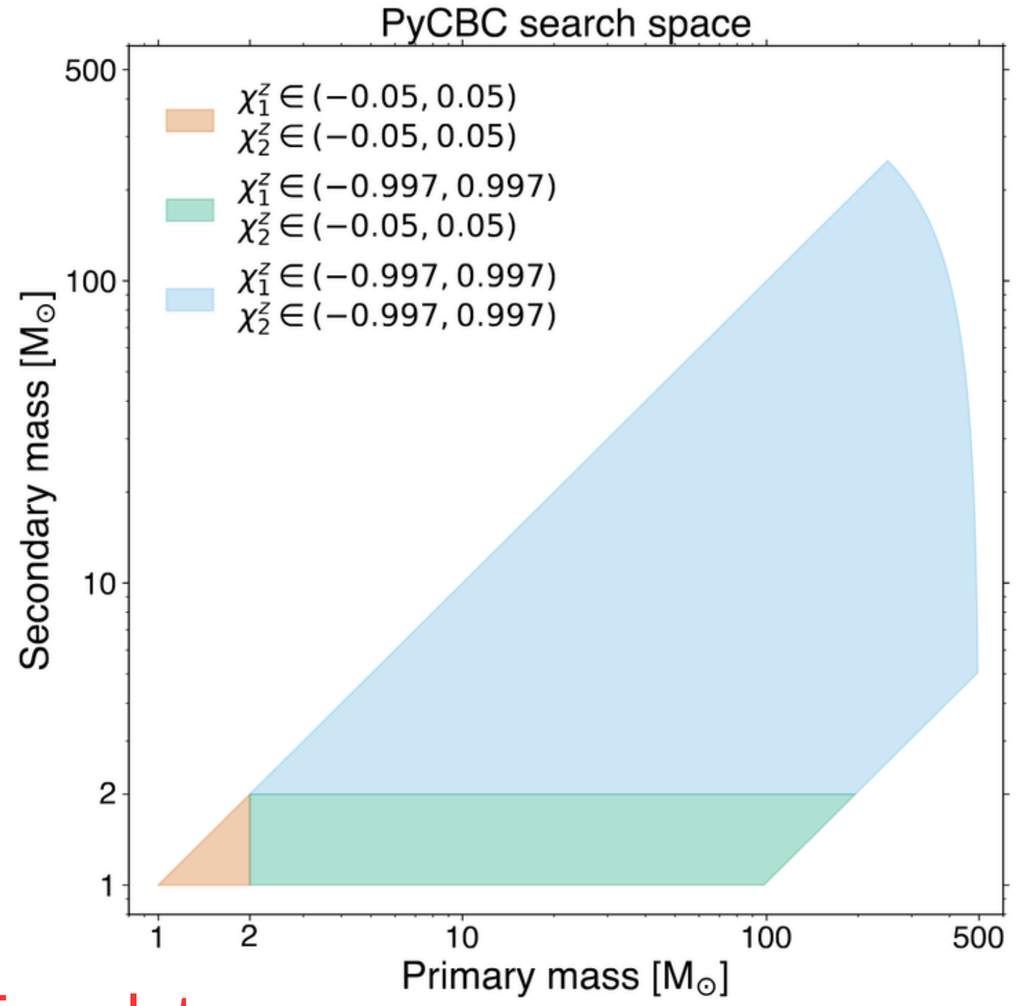

Template

GWTC-4: Methods

- Search is carried out in 2 stages:
  - Online analyses → EM follow-up
  - Offline analyses → more accuracy
- Two types of detection algorithms:
  - Pipelines not relying on waveforms
  - Pipelines relying on waveforms: matched filtering

$$\rho(t) = 4 \left| \int_{f_{\rm low}}^{f_{\rm high}} \frac{h(f) u^*(f|\boldsymbol{\theta}_{\rm int})}{S_n(f)} e^{2i\pi f t} df \right|$$

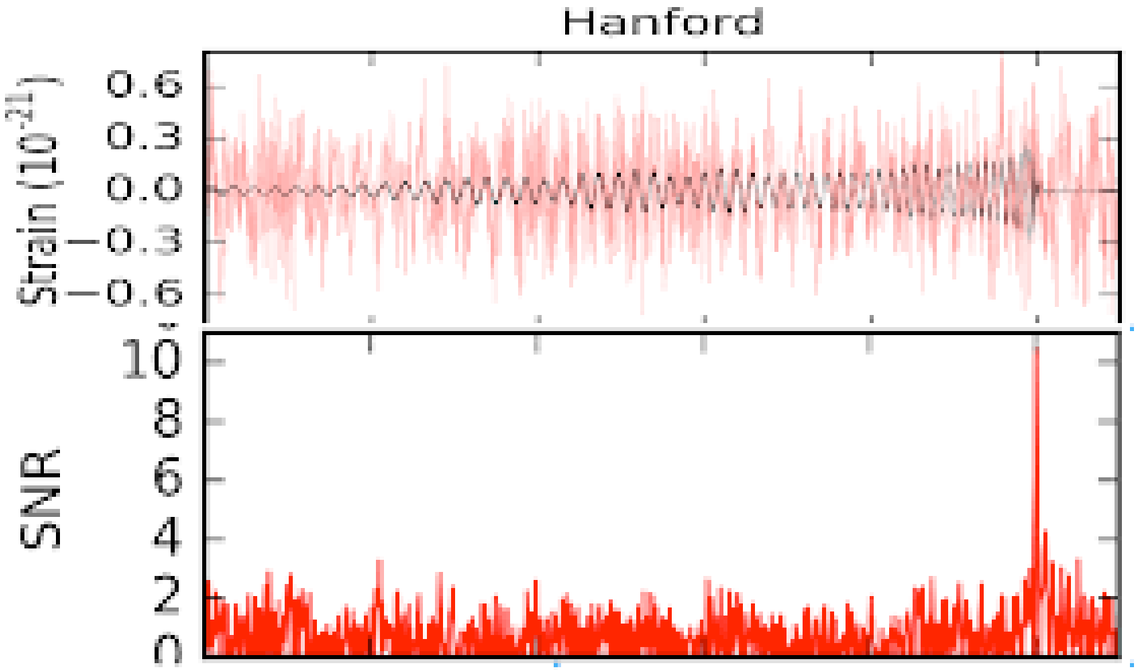

PSD of detector noise

GWTC-4: Methods

Pipelines

- Coherent WaveBurst (cWB): minimally modelled sources → coincident excess power events
- GStreamer LIGO Algorithm Library (GstLAL): time-domain matched filtering pipeline
- Multi-Band Template Analysis (MBTA): matched filtering pipeline
- PyCBC: matched filtering pipeline
- Summed Paralell Infinite Impulse Response (SPIIR): time-domain matched filtering pipeline

Pipeline	Online	Offline
cWB	Full Frames	Full Frames
GstLAL	Full Frames	Full Frames
MBTA	Full Frames	Analysis Ready
PyCBC	Full Frames	Analysis Ready
SPIIR	Full Frames	no offline analysis

LVK Collaboration, arXiv:2508.18081 (2025)

GWTC-4: Methods

LVK Collaboration, arXiv:2508.18081 (2025)

- Each pipeline assigns each candidate:
  - FAR: expected rate of non-astrophysical candidates produced with a rank (ranking statistics) at least as high as the candidate under consideration
  - p_astro: probability that a candidate is of astrophysical origin rather than of terrestrial (noise)
- Selection criteria has evolved, but now a candidate is selected if FAR < 1 / (2 days)
- Bayesian inference is performed on a 15D parameter space

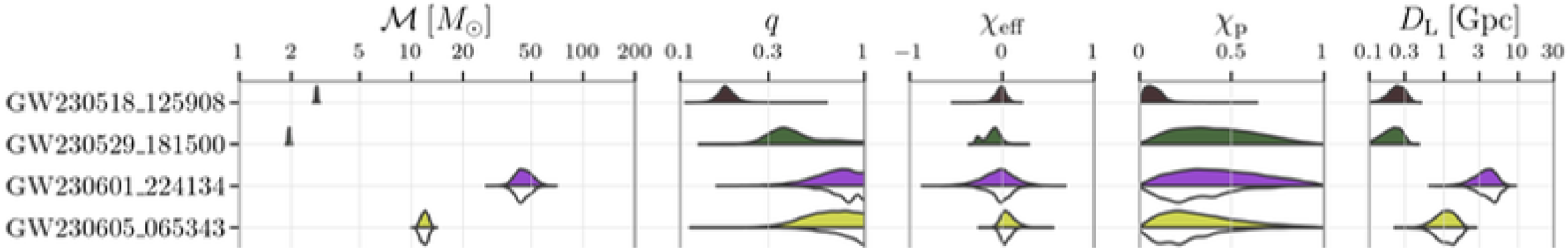

GWTC-4: Catalog updates

- O4a duration: 24/05/2024 at 3pm UTC - 16/01/2025 at 4pm UTC
- Number of CBC candidates in O4a (detected by at least 1 pipeline): 128
  - 2 of them NSBH
- No confident multimenssenger counterpart
- Total number of candidates in catalog: 90 + 128 = 218 with p_astro >= 0.5
- Candidates with FAR < 1/ year and p_astro >= 0.5 are of high-purity

LVK Collaboration, arXiv:2508.18082 (2025)

Candidate	M $[M_\odot]$	$\mathcal{M}$ $[M_\odot]$	m_1 $[M_\odot]$	m_2 $[M_\odot]$	$\chi_{\rm eff}$	$D_{\rm L}$ [Gpc]	z	$M_{\rm f}$ $[M_\odot]$	$\chi_{\rm f}$	$\Delta\Omega$ [deg^2]	SNR
GW230518_125908	$9.61^{+0.76}_{-0.79}$	$2.80^{+0.06}_{-0.06}$	$8.17^{+0.84}_{-0.92}$	$1.45^{+0.13}_{-0.10}$	$-0.01^{+0.09}_{-0.11}$	$0.24^{+0.11}_{-0.10}$	$0.05^{+0.02}_{-0.02}$	$9.46^{+0.76}_{-0.80}$	$0.38^{+0.03}_{-0.03}$	490	$14.2^{+0.2}_{-0.4}$
GW230529_181500	$5.08^{+0.61}_{-0.60}$	$1.94^{+0.04}_{-0.04}$	$3.66^{+0.82}_{-1.21}$	$1.42^{+0.60}_{-0.22}$	$-0.10^{+0.12}_{-0.18}$	$0.2^{+0.1}_{-0.1}$	$0.04^{+0.02}_{-0.02}$	$4.92^{+0.62}_{-0.63}$	$0.58^{+0.08}_{-0.06}$	24000	$11.6^{+0.3}_{-0.4}$
GW230601_224134	107^{+22}_{-15}	$45.0^{+10.0}_{-7.3}$	64^{+17}_{-13}	44^{+14}_{-15}	$-0.03^{+0.27}_{-0.32}$	$3.7^{+2.1}_{-1.8}$	$0.60^{+0.28}_{-0.26}$	102^{+21}_{-14}	$0.67^{+0.12}_{-0.13}$	3300	$12.3^{+0.2}_{-0.3}$
GW230605_065343	$28.6^{+4.0}_{-2.8}$	$11.9^{+1.0}_{-0.9}$	$17.2^{+6.5}_{-3.5}$	$11.1^{+2.5}_{-2.7}$	$0.06^{+0.16}_{-0.10}$	$1.1^{+0.6}_{-0.5}$	$0.21^{+0.10}_{-0.09}$	$27.3^{+4.1}_{-2.7}$	$0.69^{+0.05}_{-0.05}$	1000	$10.5^{+0.3}_{-0.4}$

GWTC-4: Catalog updates

- Interesting findings:
  - Some signals detected with SNR > 30. The one with highest SNR (= 42.1): GW230814_230901
  - Most massive signal: GW231123_135430 (source frame total mass: $236^{+29}_{-48}\,M_\odot$)

LVK Collaboration, arXiv:2508.18082 (2025)

Candidate	M $[M_\odot]$	$\mathcal{M}$ $[M_\odot]$	m_1 $[M_\odot]$	m_2 $[M_\odot]$	$\chi_{\rm eff}$	$D_{\rm L}$ [Gpc]	z	$M_{\rm f}$ $[M_\odot]$	$\chi_{\rm f}$	$\Delta\Omega$ [deg^2]	SNR
GW230814_061920	110^{+26}_{-20}	$45.5^{+11.9}_{-9.9}$	69^{+19}_{-17}	42^{+17}_{-16}	$0.05^{+0.29}_{-0.28}$	$4.0^{+3.4}_{-2.0}$	$0.65^{+0.42}_{-0.28}$	105^{+24}_{-19}	$0.69^{+0.12}_{-0.14}$	5200	$9.4^{+0.3}_{-0.5}$
GW230814_230901	$61.8^{+2.0}_{-2.1}$	$26.7^{+0.9}_{-1.0}$	$33.6^{+2.8}_{-2.2}$	$28.3^{+2.1}_{-3.0}$	$-0.01^{+0.06}_{-0.08}$	$0.28^{+0.17}_{-0.13}$	$0.06^{+0.04}_{-0.03}$	$58.9^{+1.9}_{-1.9}$	$0.68^{+0.02}_{-0.03}$	26000	$42.1^{+0.1}_{-0.1}$
GW230819_171910	106^{+41}_{-22}	42^{+14}_{-11}	70^{+47}_{-21}	35^{+20}_{-19}	$-0.04^{+0.36}_{-0.43}$	$4.0^{+3.9}_{-2.2}$	$0.65^{+0.49}_{-0.31}$	102^{+41}_{-22}	$0.64^{+0.19}_{-0.25}$	4800	$8.9^{+0.4}_{-0.5}$
GW231119_075248	82^{+29}_{-18}	$34.4^{+12.4}_{-7.8}$	49^{+23}_{-13}	34^{+15}_{-13}	$-0.002^{+0.279}_{-0.302}$	$6.7^{+5.5}_{-3.7}$	$0.99^{+0.62}_{-0.48}$	79^{+27}_{-18}	$0.68^{+0.11}_{-0.16}$	5900	$7.7^{+0.3}_{-0.5}$
GW231123_135430	236^{+29}_{-48}	101^{+13}_{-30}	137^{+23}_{-18}	101^{+22}_{-51}	$0.3^{+0.2}_{-0.4}$	$2.2^{+2.0}_{-1.5}$	$0.39^{+0.28}_{-0.25}$	222^{+27}_{-42}	$0.84^{+0.07}_{-0.19}$	1700	$20.7^{+0.2}_{-0.3}$
GW231127_165300	74^{+22}_{-15}	$30.5^{+9.5}_{-6.7}$	45^{+18}_{-12}	29^{+12}_{-12}	$0.05^{+0.30}_{-0.32}$	$4.5^{+3.6}_{-2.5}$	$0.71^{+0.44}_{-0.35}$	71^{+21}_{-14}	$0.69^{+0.12}_{-0.17}$	4400	$8.3^{+0.3}_{-0.5}$

GWTC-4: CBC population updates

LVK Collaboration, arXiv:2508.18083 (2025)

- To update the CBC pops properties: 161 CBC candidates have been used (FAR < 1 / year)
- Merger rates:
  - BBH: 14 - $26\ \mathrm{Gpc^{-3}\ yr^{-1}}$
  - BNS: $7.6\text{–}250\ \mathrm{Gpc^{-3}\ yr^{-1}}$
  - NSBH: $9.1\text{–}84\ \mathrm{Gpc^{-3}\ yr^{-1}}$

- Mass gap between NSs and BBHs is supported by EM observations
  - However, a completely empty mass gap between NSs and BHs is disfavoured
  - We cannot rule out existence of very narrow gaps
- Existence of an upper mass gap between 45-120 solar masses: consistent with theorized pair instability mass gap

GWTC–4: BBH population properties – mass ratio

- Mass ratio distribution can be described by a power law with an index $\beta_q = 1.2^{+1.2}_{-1.0}$
- BHs with masses ~ 35 Msol preferentially merge with BHs of = mass (favoured by most formation channels)
- BHs with masses ~ 10 Msol preferentially merge with lighter BHs

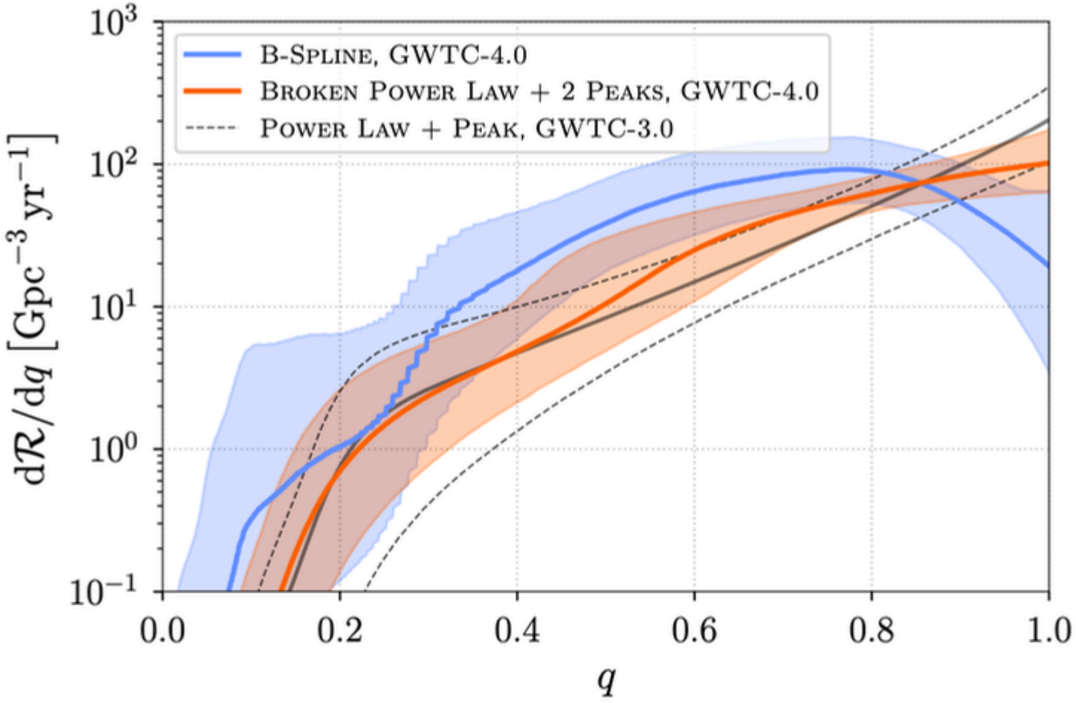

LVK Collaboration, arXiv:2508.18083 (2025)

GWTC–4: BBH population properties – spin

LVK Collaboration, arXiv:2508.18083 (2025)

- Spin magnitude distribution has support at 0
- At least one binary has spin > 0
- Spin tilt distribution may peak away from perfect alignment with the orbital angular momentum (between 20-40% has spins more than 90 degrees misaligned with the orbital angular momentum)
- The effective spin distribution is assymmetric about its peak (0)

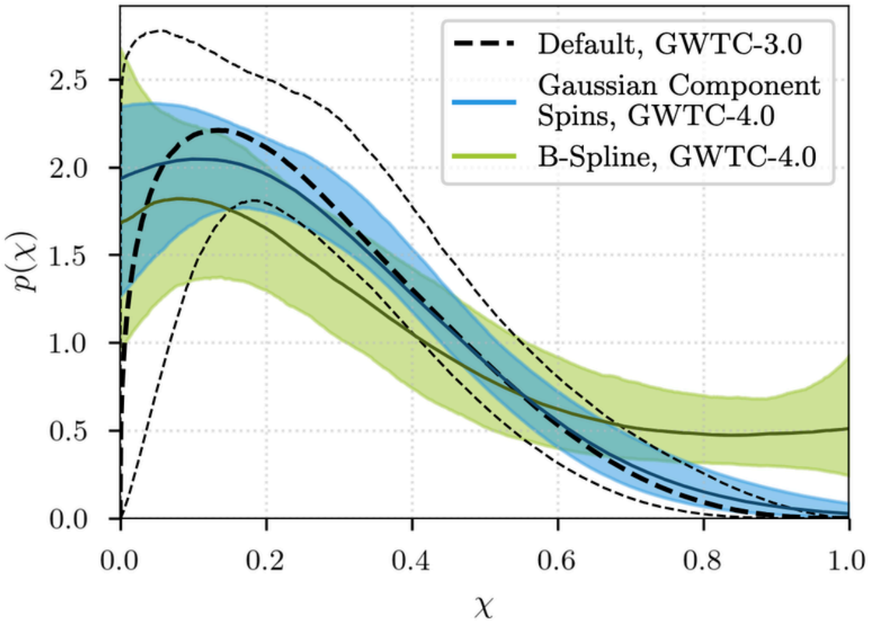

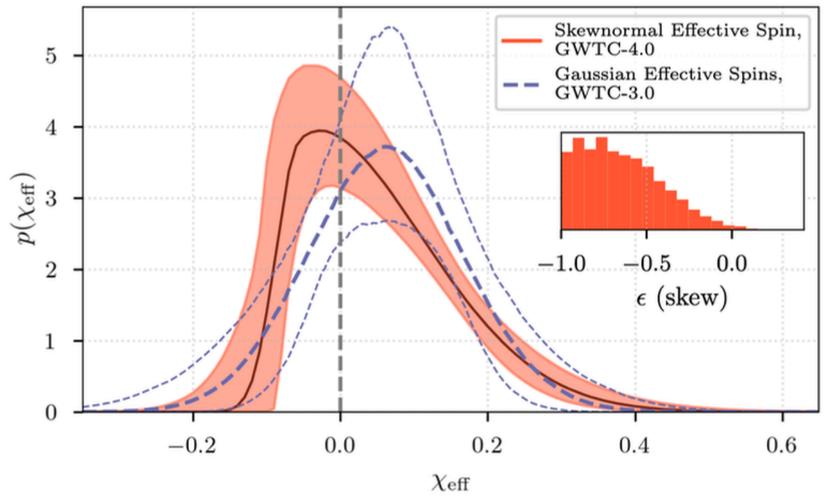

GWTC–4: BBH population properties – merger rate

BBH merger rate at z = 0.2 is

$$\mathbf{29^{+8.5}_{-6.5}\,Gpc^{-3}\,yr^{-1}}$$

BBH merger rate evolution as a function of z consistent with star formation rate density

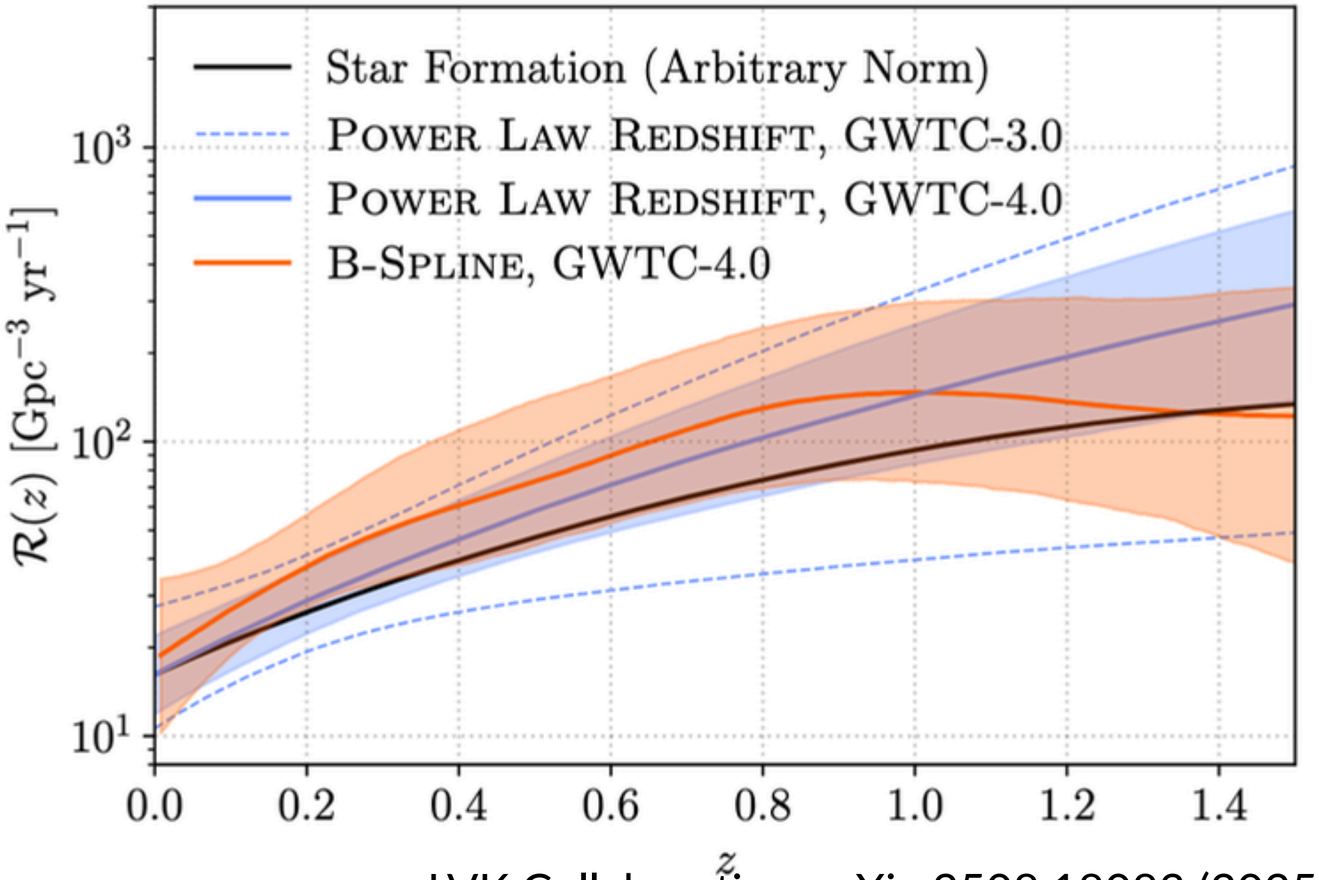

LVK Collaboration, arXiv:2508.18083 (2025)

GWTC–4: BBH population properties – mass

LVK Collaboration, arXiv:2508.18083 (2025)

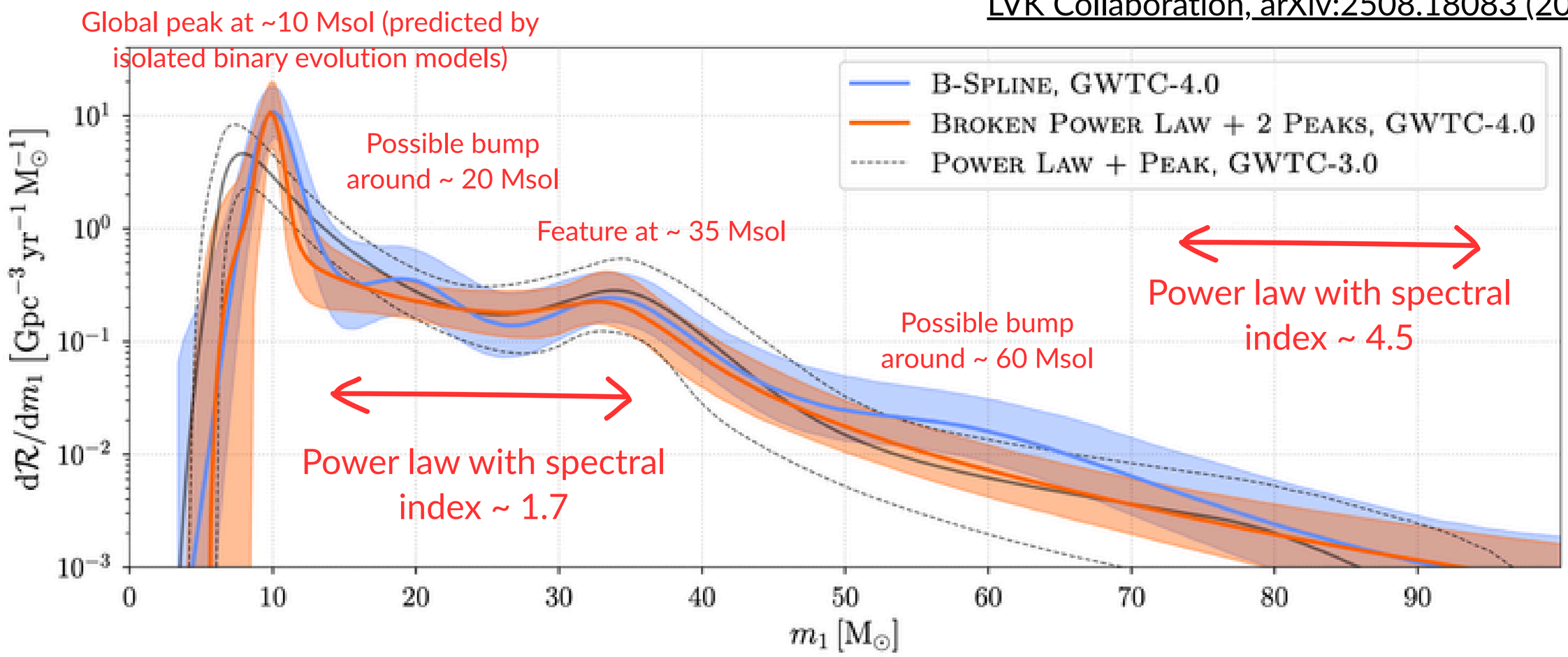

GWTC–4: BBH population properties – mass

LVK Collaboration, arXiv:2508.18083 (2025)

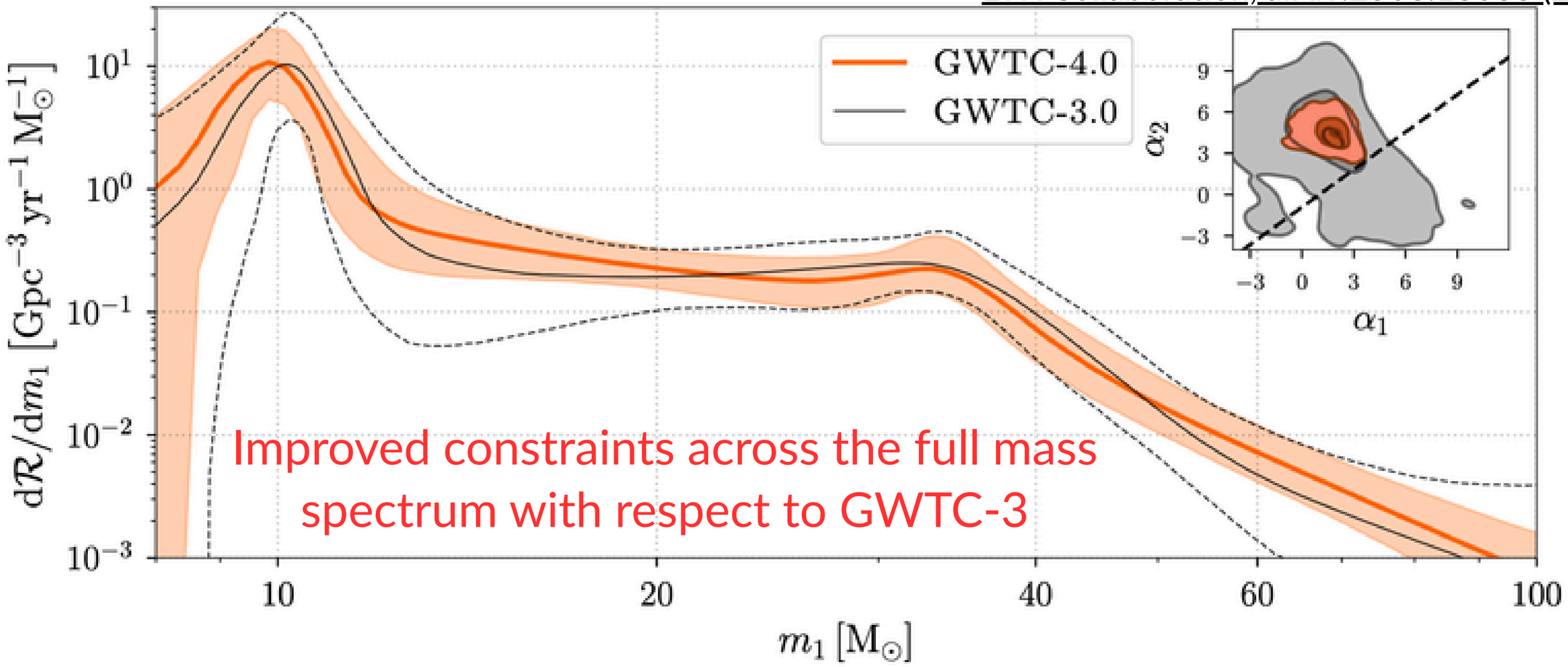

O1-O4a LVK results on the search for an isotropic GWB

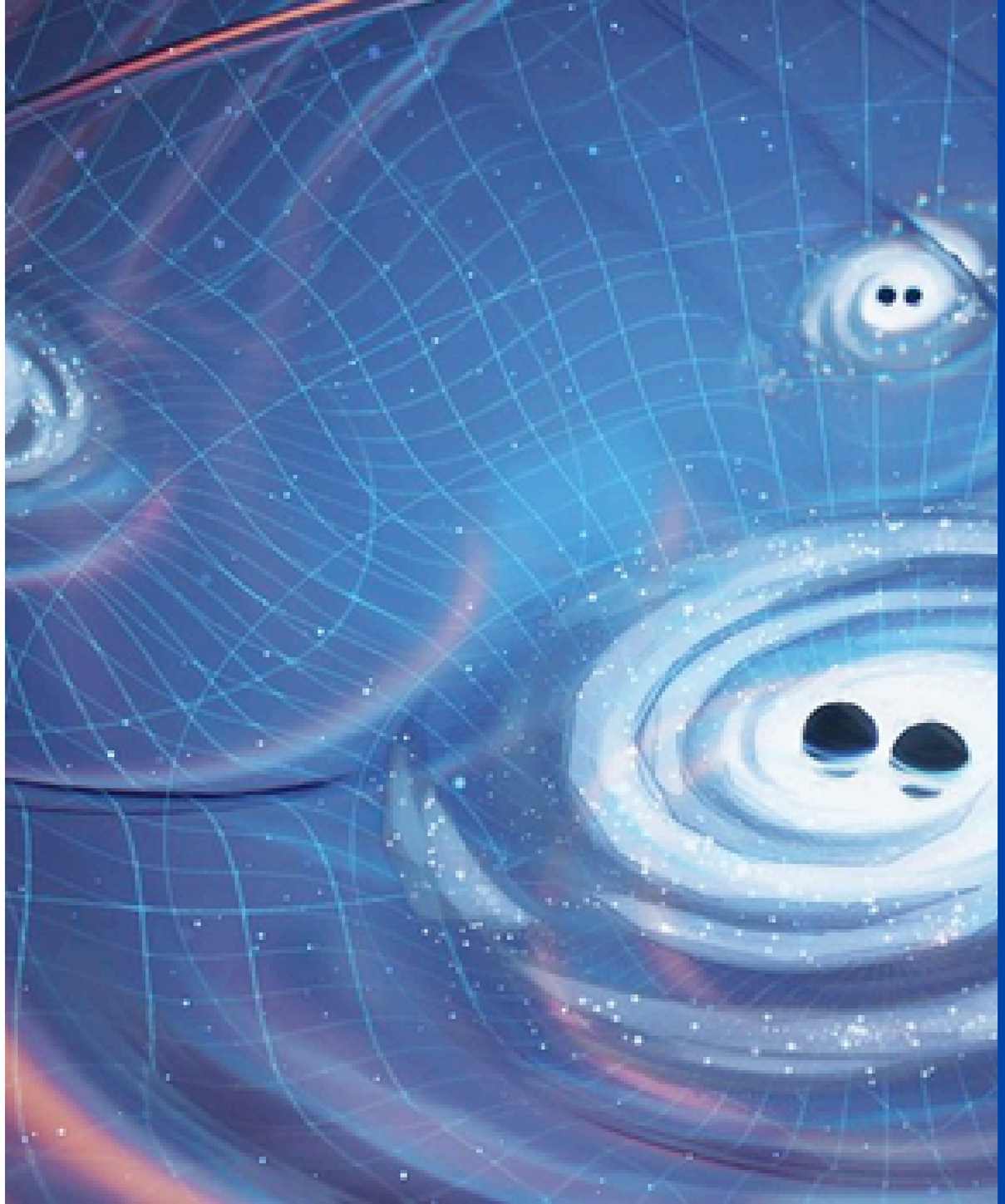

Gravitational wave background

Superposition of random GW signals produced by a large number of weak, independent and unresolved sources

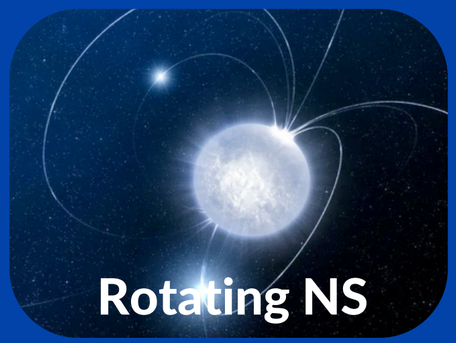

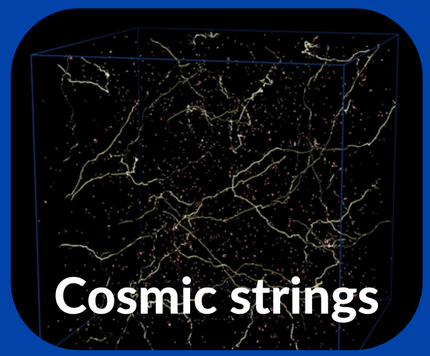

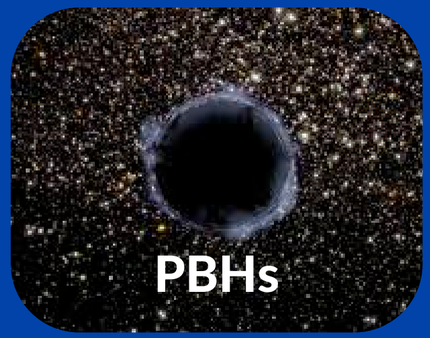

GWB characterization

- Statistically: probability distribution or moments
- Large number of independent sources: GWB is Gaussian

$$\langle h_{ab}(t,\vec{x})\rangle, \quad \langle h_{ab}(t,\vec{x})h_{cd}(t',\vec{x}')\rangle$$

Assumptions

- Isotropic
- Stationary
- Unpolarized
- Gaussian

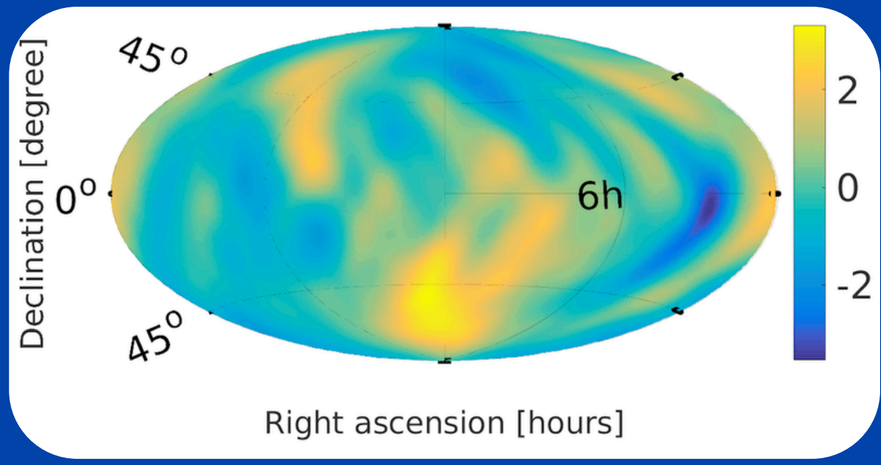

$$\left\langle h_A(f,\hat{n})h^*_{A'}(f',\hat{n}')\right\rangle = \frac{1}{16\pi}S_h(f)\delta(f-f')\delta_{AA'}\delta^2(\hat{n},\hat{n}')$$

GWB characterization

Fractional energy density spectrum in GWs

$$\Omega_{\rm gw}(f) = \frac{1}{\rho_c}\frac{d\rho_{\rm gw}}{d\ln f}$$

$$\rho_{\rm GW} = \frac{c^2}{32\pi G}\langle \dot{h}_{ab}(t,\mathbf{x})\dot{h}^{ab}(t,\mathbf{x})\rangle$$

$$\Omega_{\rm GW}(f) = \frac{2\pi^2}{3H_0^2} f^3 S_h(f)$$

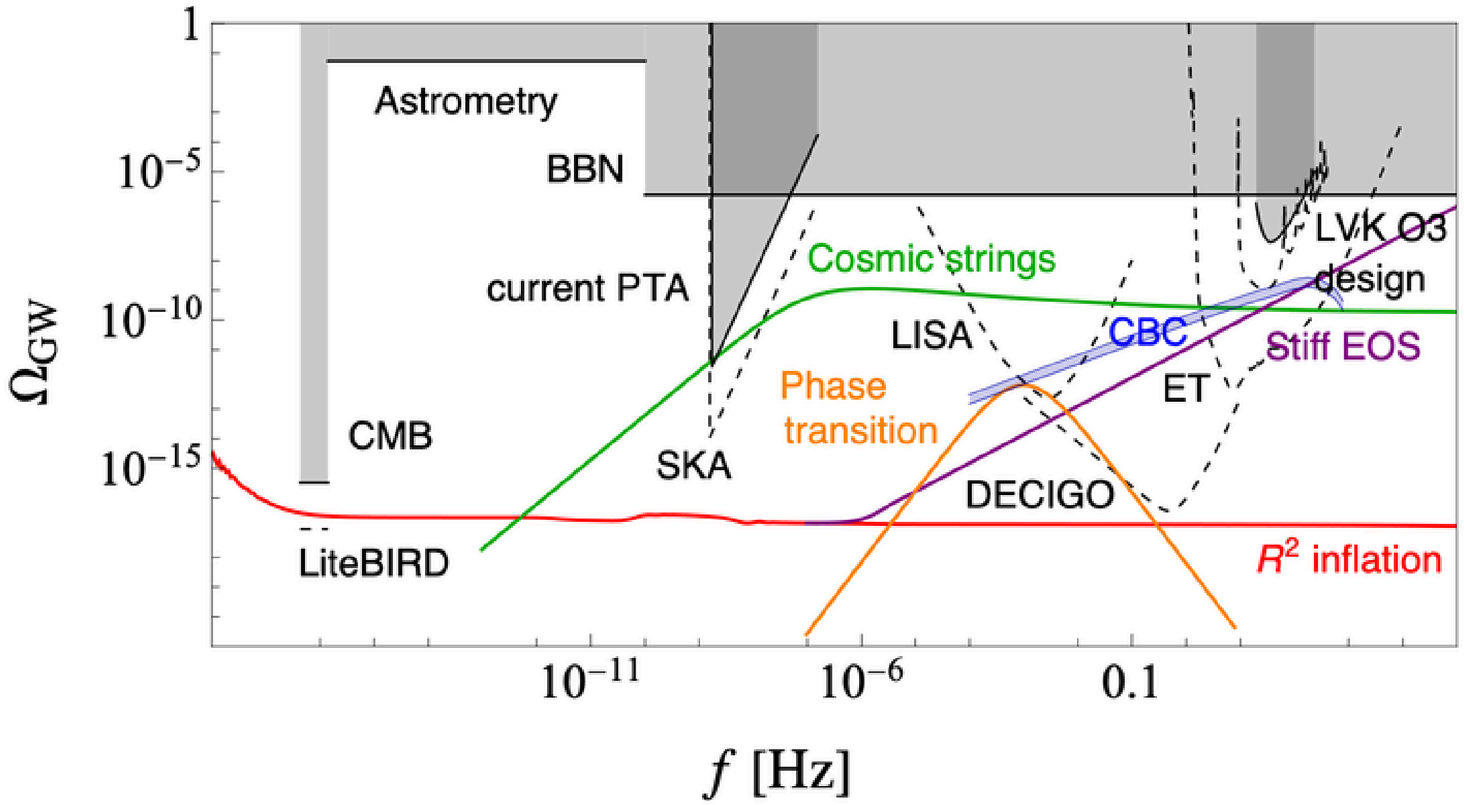

ARR, and S. Kuroyanagi. 2024. *Primordial Black Holes*. Chap. 27. Springer (link). Arxiv: https://doi.org/10.48550/arXiv.2407.00205.

LVK search for an isotropic GWB

Hybrid search → Frequentist
Hybrid search → Bayesian

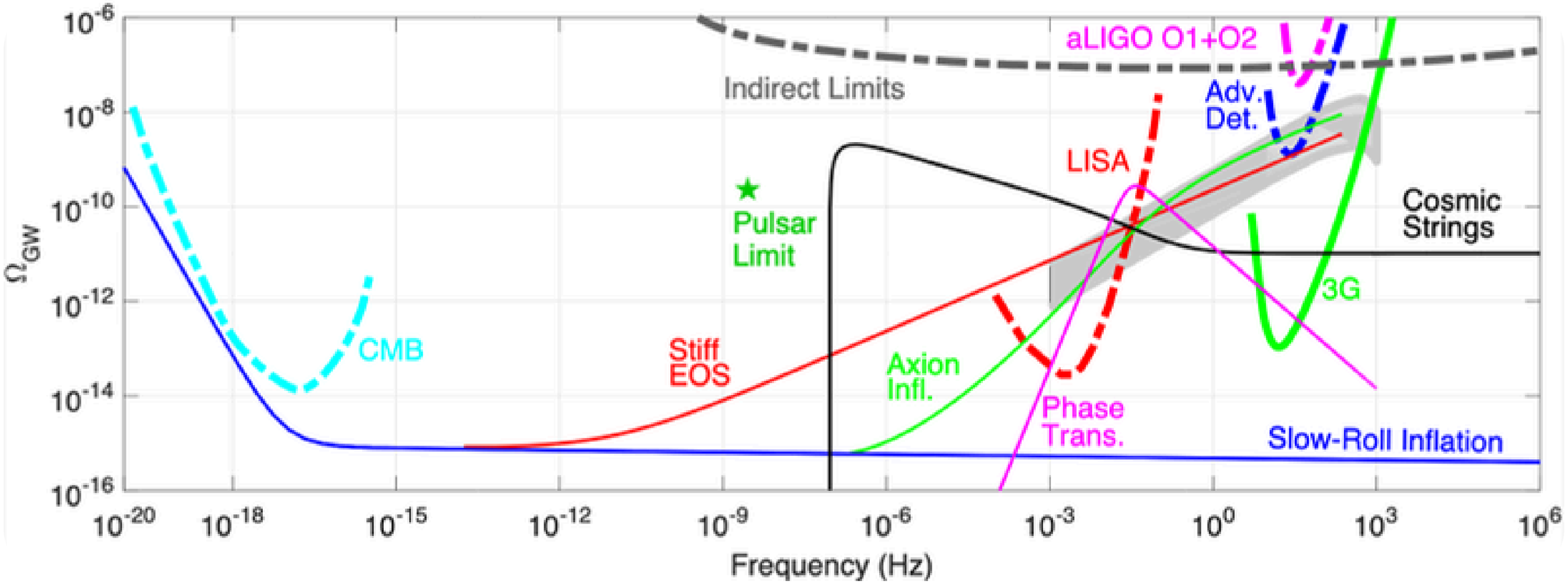

LVK search for an isotropic GWB

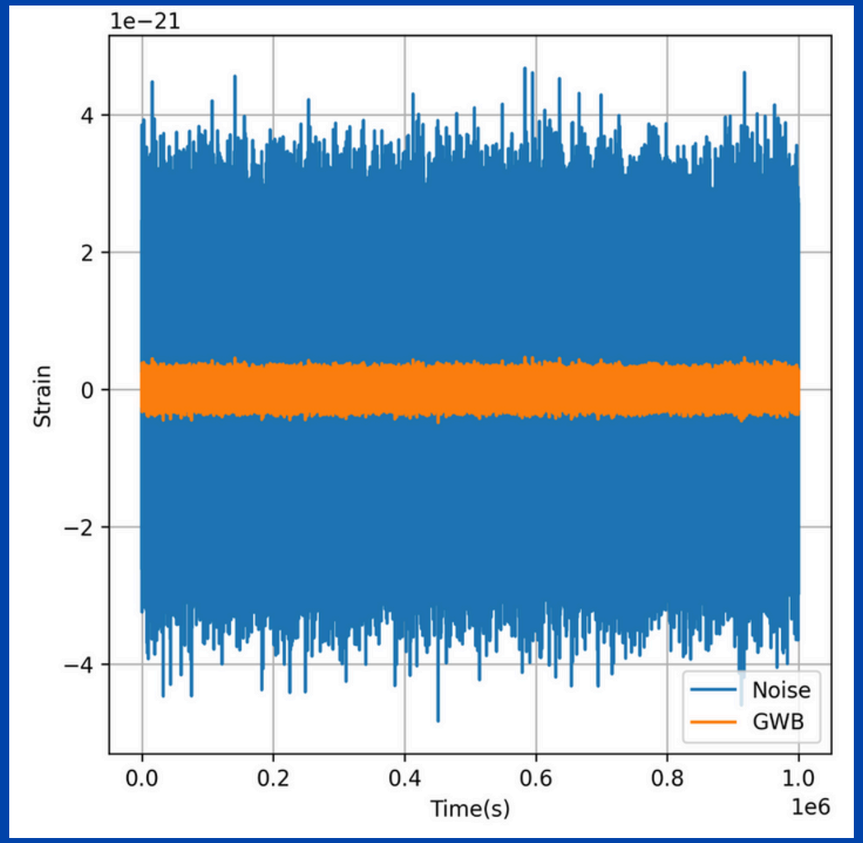

Cross correlation search

$$s_1(t) = n_1(t) + h_1(t),$$
$$s_2(t) = n_2(t) + h_2(t)\,.$$

$$\langle s_1^*(f)\, s_2(f') \rangle$$

LVK search for an isotropic GWB

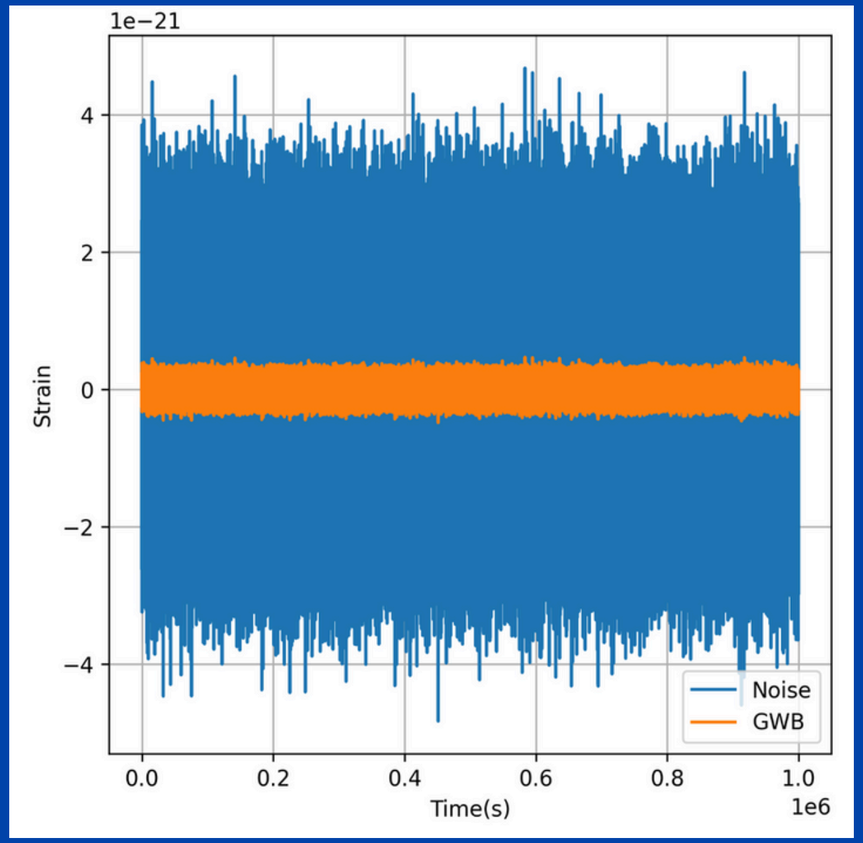

Cross correlation search

$$s_1(t) = n_1(t) + h_1(t),$$
$$s_2(t) = n_2(t) + h_2(t)\,.$$

$$\langle s_1^*(f)\, s_2(f') \rangle$$

$$\langle n_i^*(f)\, h_j(f') \rangle = 0$$

$$\langle n_i^*(f)\, n_j(f') \rangle = \delta_{ij}$$

LVK search for an isotropic GWB

$$\langle s_1^*(f)\, s_2(f') \rangle$$

Cross correlation estimator and variance

$$\hat{C}^{IJ}(f) = \frac{2}{T} \frac{\mathrm{Re}[\tilde{s}_I^\star(f)\tilde{s}_J(f)]}{\gamma_{IJ}(f) S_0(f)}$$

$$\sigma^2_{IJ}(f) \approx \frac{1}{2T\Delta f} \frac{P_I(f) P_J(f)}{\gamma^2_{IJ}(f) S_0^2(f)}$$

LVK search for an isotropic GWB

Cross correlation spectrum (frequentist analysis)

$$\hat{C}^{IJ}(f) = \frac{2}{T} \frac{\mathrm{Re}[\tilde{s}_I^\star(f)\tilde{s}_J(f)]}{\gamma_{IJ}(f)S_0(f)}$$

$$\sigma^2_{IJ}(f) \approx \frac{1}{2T\Delta f} \frac{P_I(f)P_J(f)}{\gamma^2_{IJ}(f)S_0^2(f)}$$

LVK search for an isotropic GWB

Cross correlation spectrum (frequentist analysis)

$$\hat{C}^{IJ}(f) = \frac{2\ \mathrm{Re}[\tilde{s}_I^{\star}(f)\tilde{s}_J(f)]}{T\ \gamma_{IJ}(f)S_0(f)}$$

$$\sigma^2_{IJ}(f) \approx \frac{1}{2T\Delta f}\frac{P_I(f)P_J(f)}{\gamma^2_{IJ}(f)S_0^2(f)}$$

T : observation time

LVK search for an isotropic GWB

Cross correlation spectrum (frequentist analysis)

$$\hat{C}^{IJ}(f) = \frac{2}{T}\frac{\mathrm{Re}[\tilde{s}_I^{\star}(f)\tilde{s}_J(f)]}{\gamma_{IJ}(f)S_0(f)}$$

$$\sigma^2_{IJ}(f) \approx \frac{1}{2T\Delta f}\frac{P_I(f)P_J(f)}{\gamma^2_{IJ}(f)S_0^2(f)}$$

Overlap reduction function (ORF)

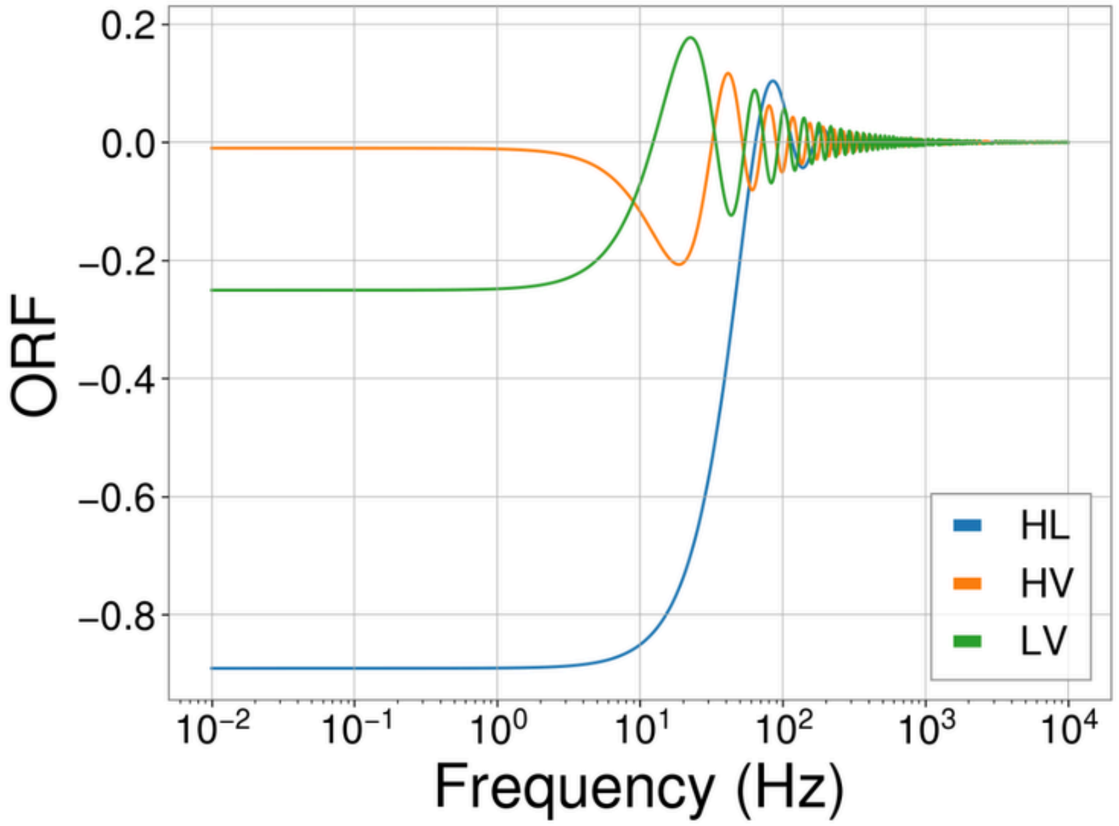

LVK search for an isotropic GWB

Cross correlation spectrum (frequentist analysis)

$$\hat{C}^{IJ}(f) = \frac{2}{T}\frac{\mathrm{Re}[\tilde{s}_I^{\star}(f)\tilde{s}_J(f)]}{\gamma_{IJ}(f)S_0(f)}$$

$$\sigma^2_{IJ}(f) \approx \frac{1}{2T\Delta f}\frac{P_I(f)P_J(f)}{\gamma^2_{IJ}(f)S_0^2(f)}$$

Noise power spectra

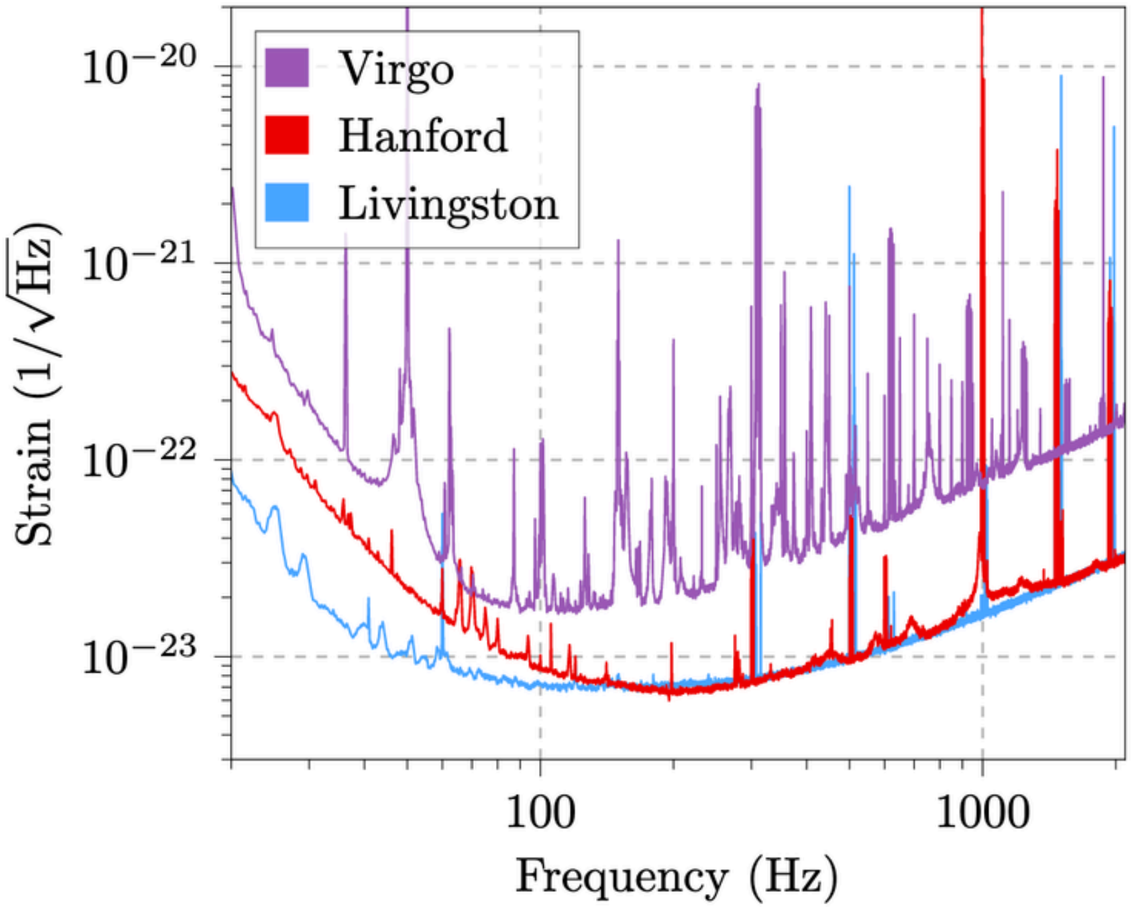

B. P. Abbott et al. (LVK), Phys. Rev. Lett. 119, 141101

LVK search for an isotropic GWB

Signal to noise ratio

$$\mathrm{SNR} = \frac{3H_0^2\sqrt{T}}{10\pi^2}\left(\int_{-\infty}^{\infty} \mathrm{d}f \, \frac{\Omega_{\mathrm{GW}}^2(|f|)\gamma_{12}^2(|f|)}{|f|^6 P_1(|f|)P_2(|f|)}\right)^{1/2}$$

LVK search for an isotropic GWB

Signal to noise ratio

$$\mathrm{SNR} = \frac{3H_0^2\sqrt{T}}{10\pi^2}\left(\int_{-\infty}^{\infty} \mathrm{d}f \, \frac{\Omega_{\mathrm{GW}}^2(|f|)\gamma_{12}^2(|f|)}{|f|^6 P_1(|f|)P_2(|f|)}\right)^{1/2}$$

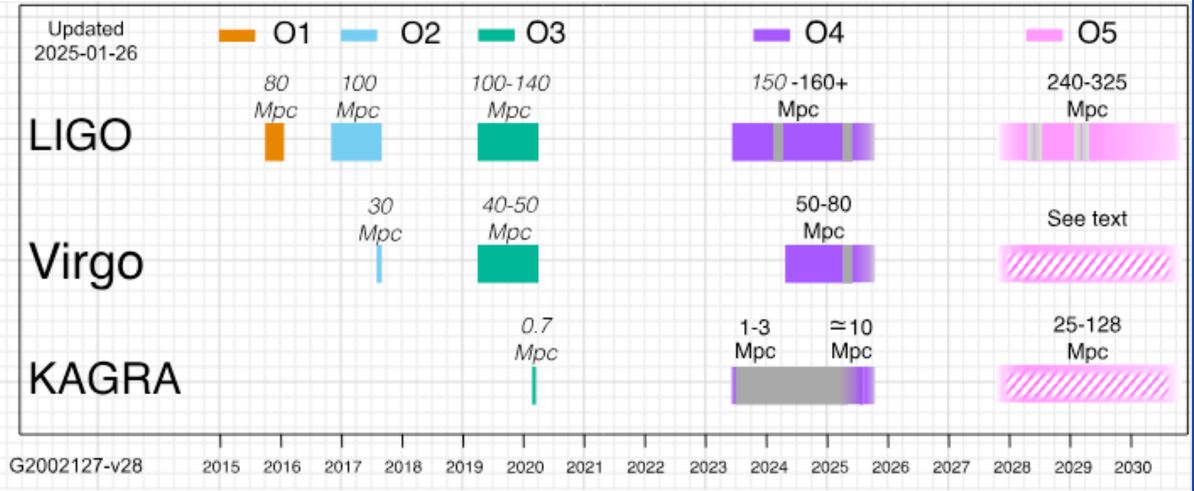

LVK search for an isotropic GWB

Signal to noise ratio

$$\mathrm{SNR} = \frac{3H_0^2\sqrt{T}}{10\pi^2}\left(\int_{-\infty}^{\infty} \mathrm{d}f \frac{\Omega_{\mathrm{GW}}^2(|f|)\gamma_{12}^2(|f|)}{|f|^6 P_1(|f|)P_2(|f|)}\right)^{1/2}$$

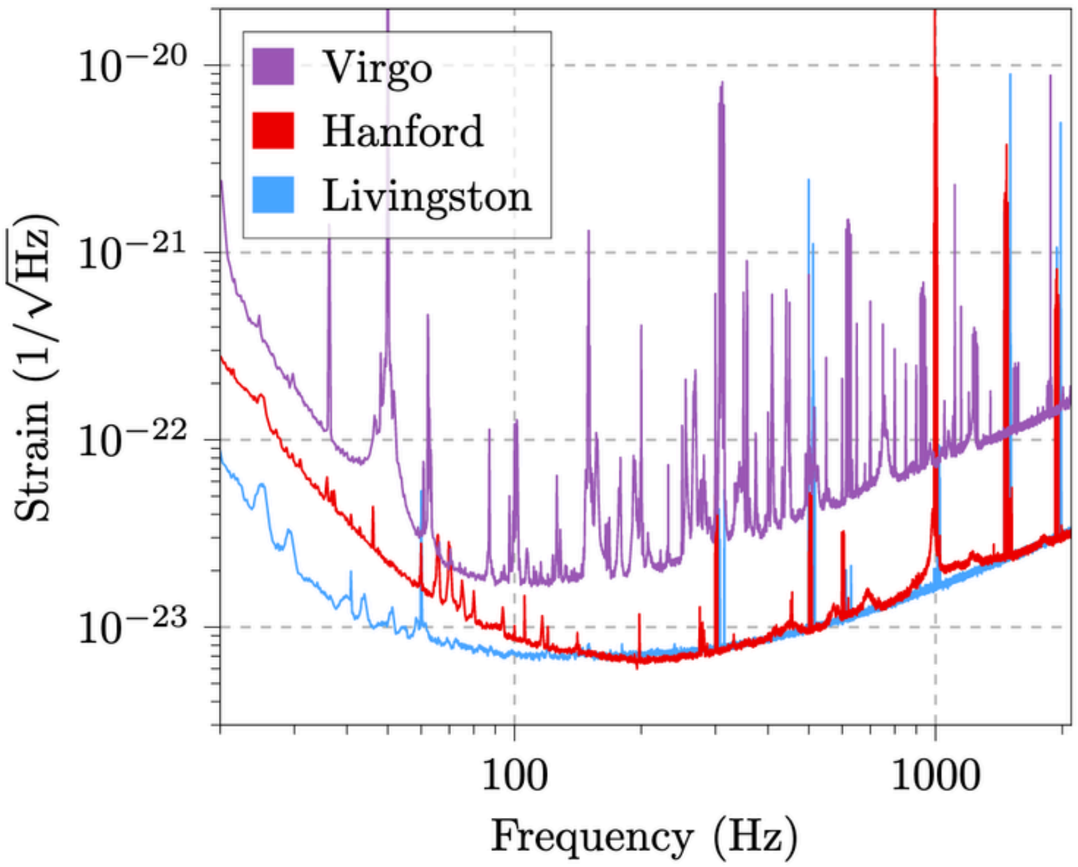

LVK search for an isotropic GWB

Signal to noise ratio

$$\mathrm{SNR} = \frac{3H_0^2\sqrt{T}}{10\pi^2}\left(\int_{-\infty}^{\infty} \mathrm{d}f\, \frac{\Omega_{\mathrm{GW}}^2(|f|)\gamma_{12}^2(|f|)}{|f|^6 P_1(|f|)P_2(|f|)}\right)^{1/2}$$

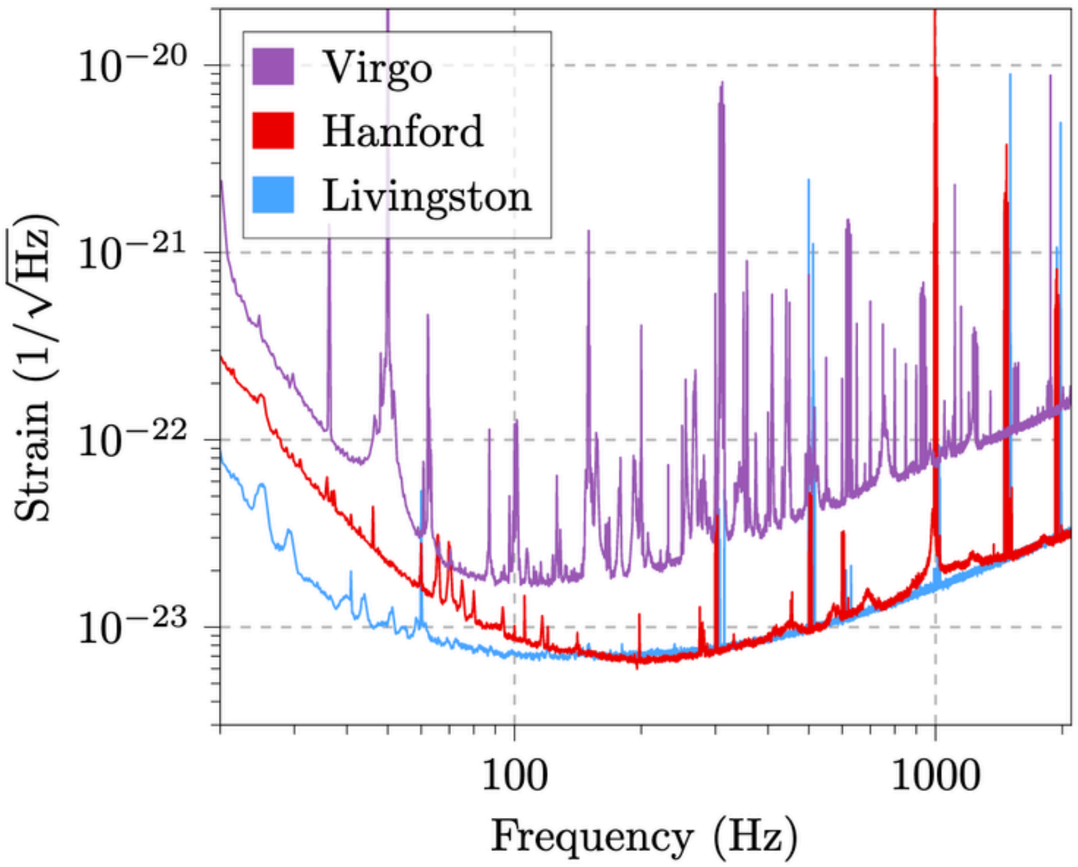

LVK search for an isotropic GWB

Signal to noise ratio

$$\mathrm{SNR} = \frac{3H_0^2\sqrt{T}}{10\pi^2}\left(\int_{-\infty}^{\infty} \mathrm{d}f \frac{\Omega_{\mathrm{GW}}^2(|f|)\gamma_{12}^2(|f|)}{|f|^6 P_1(|f|)P_2(|f|)}\right)^{1/2}$$

$$\Omega_{\mathrm{GW}}(f) = \Omega_\alpha \left(\frac{f}{f_{\mathrm{ref}}}\right)^\alpha$$

- $f$ref = 25 Hz
- α = 0 : inflation, cosmic strings
- α = 2/3 : inspiral phase of CBCs
- α = 3 : supernovae

LVK search for an isotropic GWB

Gaussian likelihood

$$p(\hat{\Omega}_0|\Theta,\Lambda) \propto \exp\left[-\frac{1}{2}\sum_f \frac{(\hat{\Omega}_0(f) - \Lambda\Omega_{\rm GW}(f;\Theta))^2}{\sigma_0^2(f)}\right]$$

LVK search for an isotropic GWB

Gaussian likelihood

$$p(\hat{\Omega}_0|\Theta,\Lambda) \propto \exp\left[-\frac{1}{2}\sum_f \frac{(\hat{\Omega}_0(f) - \Lambda\Omega_{\rm GW}(f;\Theta))^2}{\sigma_0^2(f)}\right]$$

Frequentist results

LVK search for an isotropic GWB

Gaussian likelihood

$$p(\hat{\Omega}_0|\Theta,\Lambda) \propto \exp\left[-\frac{1}{2}\sum_f \frac{(\hat{\Omega}_0(f)-\Lambda\Omega_{\rm GW}(f;\Theta))^2}{\sigma_0^2(f)}\right]$$

Frequentist versus Bayesian analyses: Cross-correlation as an approximate sufficient statistic for LIGO-Virgo stochastic background searches

AM and JR, Phys. Rev. D 103, 062003

LVK search for an isotropic GWB

Gaussian likelihood

$$p(\hat{\Omega}_0|\Theta,\Lambda) \propto \exp\left[-\frac{1}{2}\sum_f \frac{(\hat{\Omega}_0(f) - \Lambda\Omega_{\rm GW}(f;\Theta))^2}{\sigma_0^2(f)}\right]$$

Model assumed to describe the GWB

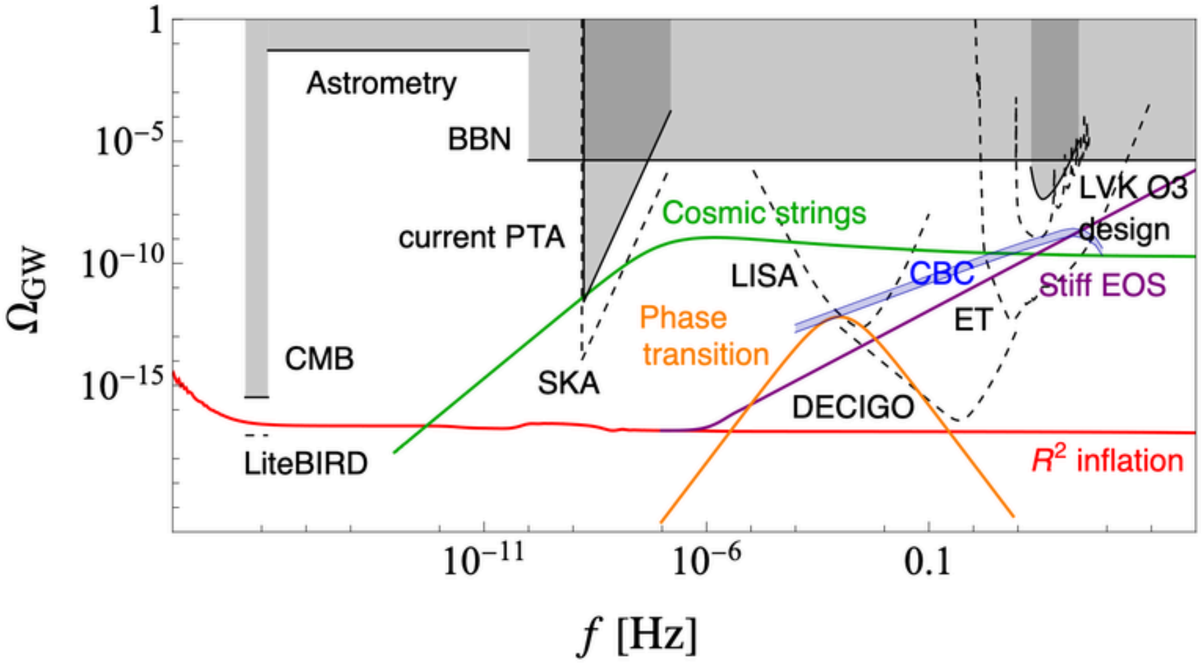

ARR, and S. Kuroyanagi. 2024. *Primordial Black Holes*. Chap. 27. Springer (link). Arxiv: https://doi.org/10.48550/arXiv.2407.00205.

Current LVK results

- H1, L1 data from O1-O4a
- Total coincident time ~ 126.57 days → 108.41 days of viable data after DQ cuts
- Frequency range of analysis: 20-1726Hz
- Pipeline: pygwb (A. R. et al 2023 ApJ 952 25)

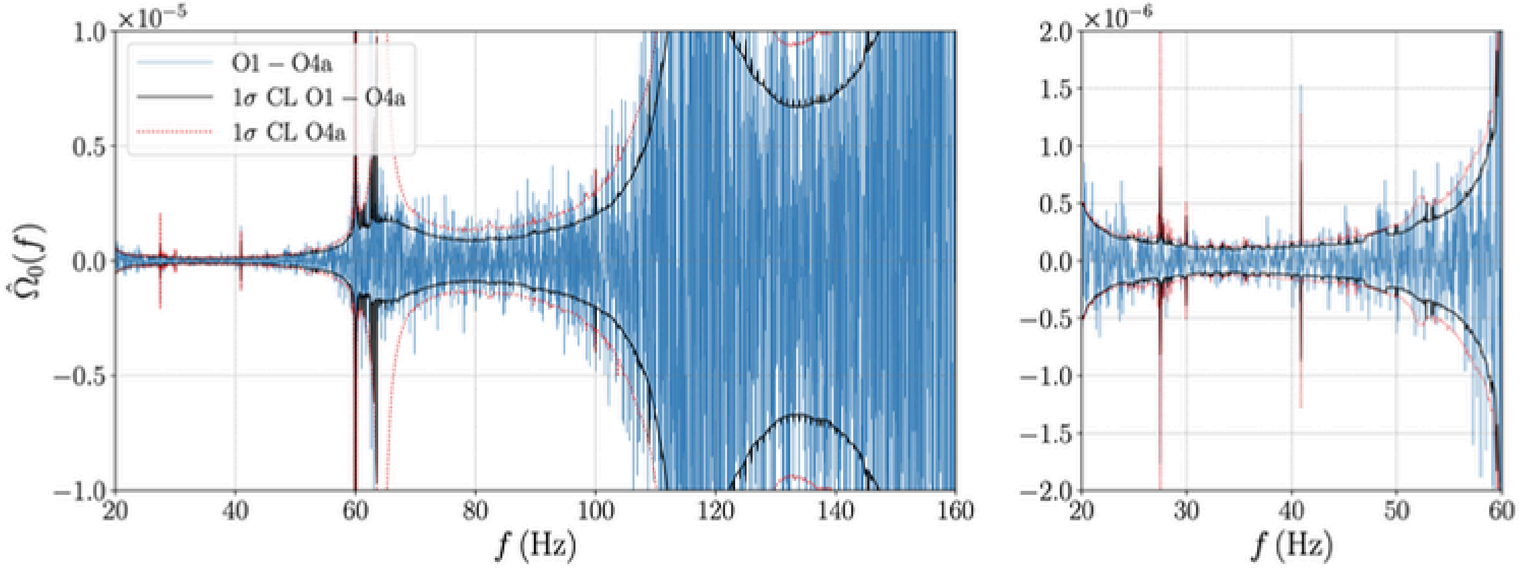

Power law	$f^{O4a}_{99\%}$ [Hz]	$\hat{\Omega}^{O4a}/10^{-9}$	$f^{O1-O4a}_{99\%}$ [Hz]	$\hat{\Omega}^{O1-O4a}/10^{-9}$
0	54.8	-2.2 ± 5.8	58.2	-1.3 ± 4.7
2/3	83.6	-1.6 ± 4.5	86.8	-1.2 ± 3.5
3	376.7	-0.1 ± 0.8	336.6	-0.3 ± 0.6

LVK Collaboration, arXiv:2508.20721 (2025)

Current LVK results

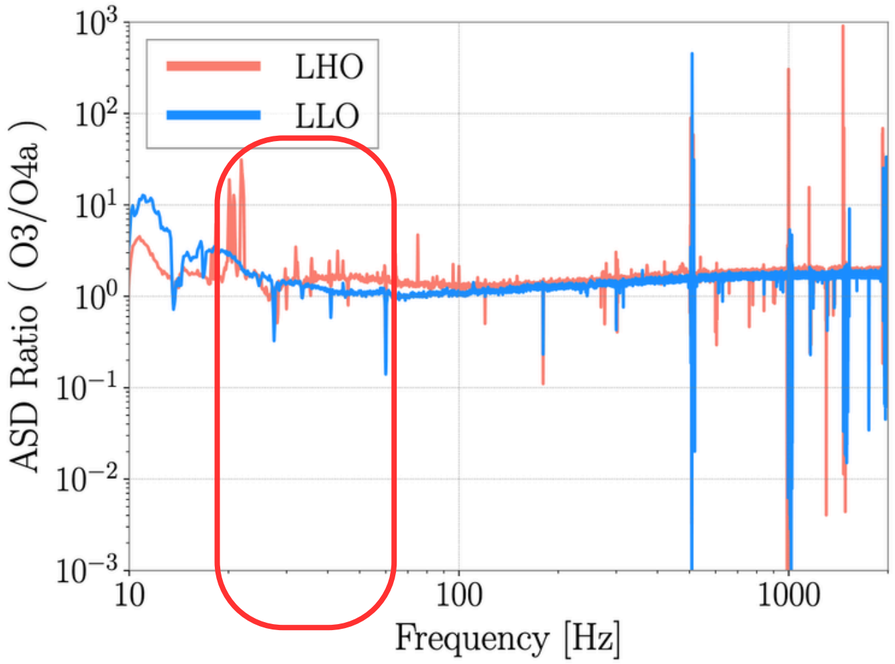

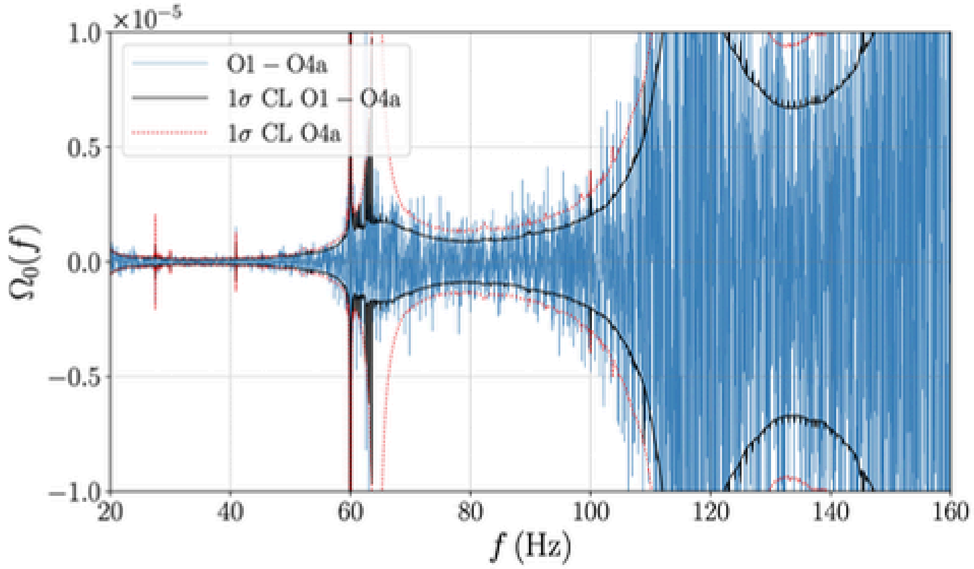

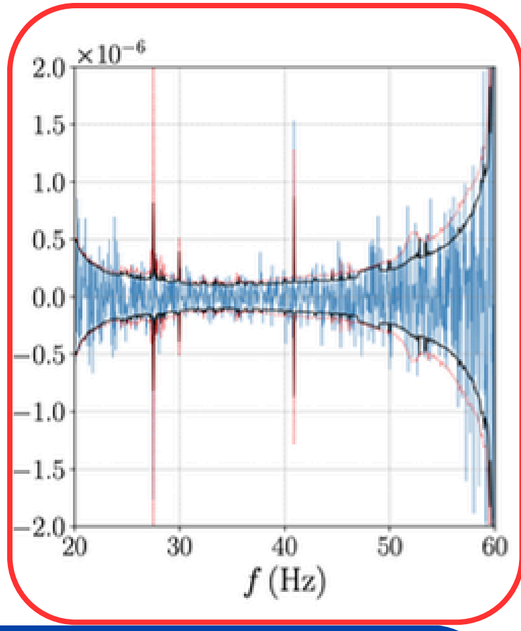

Power law	$f_{99\%}^{O4a}$ [Hz]	$\hat{\Omega}^{O4a}/10^{-9}$	$f_{99\%}^{O1-O4a}$ [Hz]	$\hat{\Omega}^{O1-O4a}/10^{-9}$
0	54.8	-2.2 ± 5.8	58.2	-1.3 ± 4.7
2/3	83.6	-1.6 ± 4.5	86.8	-1.2 ± 3.5
3	376.7	-0.1 ± 0.8	336.6	-0.3 ± 0.6

LVK Collaboration, arXiv:2508.20721 (2025)

Current LVK results – Bayesian

$$\Omega_{\rm GW}(f) = \Omega_\alpha F_\alpha(f)\,, \qquad F_\alpha(f) = \left(\frac{f}{25\,\mathrm{Hz}}\right)^\alpha$$

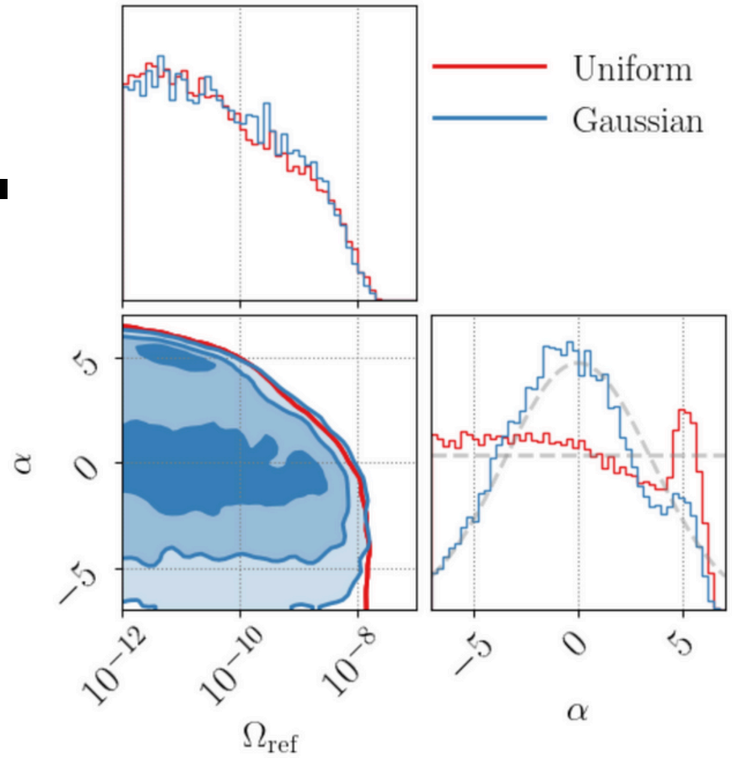

Upper limits at 95% CL

	Log-uniform prior		
α	O1-O4a	O1-O3	Improvement
0	2.8×10^{-9}	5.8×10^{-9}	2.1
2/3	2.0×10^{-9}	3.4×10^{-9}	1.7
3	3.2×10^{-10}	3.9×10^{-10}	1.2
Marginalized	2.9×10^{-9}	6.6×10^{-9}	2.3

LVK Collaboration, arXiv:2508.20721 (2025)

Current LVK results – Bayesian

$$\Omega_{\rm GW}(f) = \Omega_\alpha F_\alpha(f)\,, \qquad F_\alpha(f) = \left(\frac{f}{25\,\mathrm{Hz}}\right)^\alpha$$

Upper limits at 95% CL

	Log-uniform prior		
α	O1-O4a	O1-O3	Improvement
0	2.8×10^{-9}	5.8×10^{-9}	2.1
2/3	2.0×10^{-9}	3.4×10^{-9}	1.7
3	3.2×10^{-10}	3.9×10^{-10}	1.2
Marginalized	2.9×10^{-9}	6.6×10^{-9}	2.3

LVK Collaboration, arXiv:2508.20721 (2025)

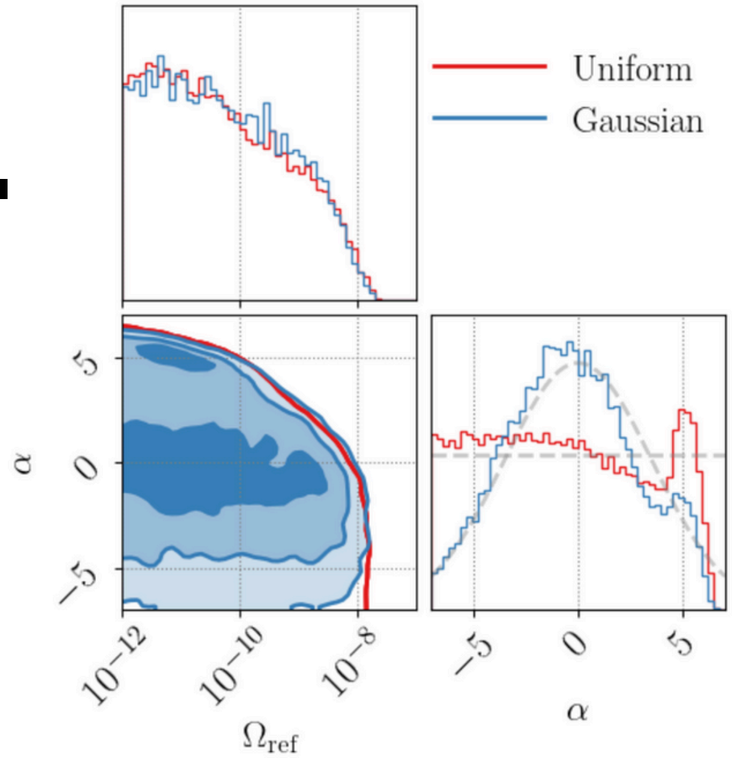

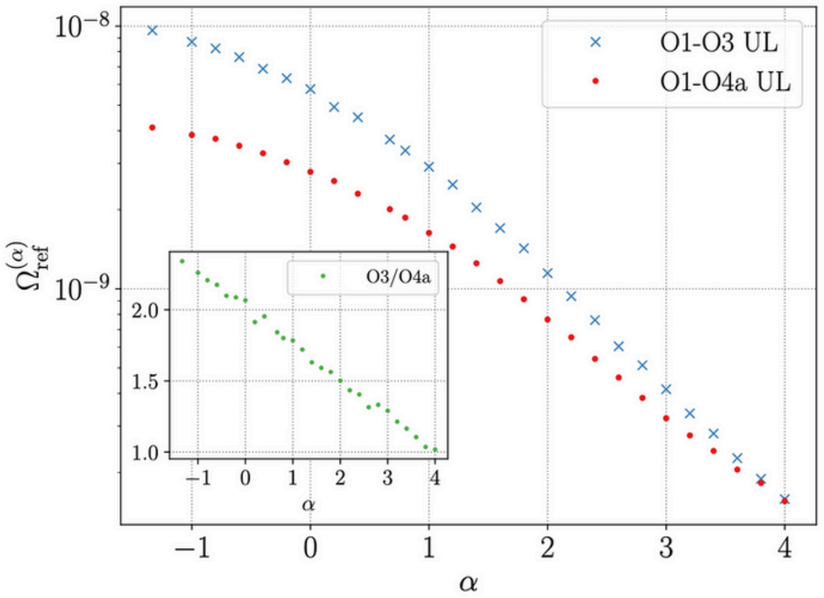

Current LVK results – constraints on non-GR pols

- Signal may include vector, scalar and tensor polarizations
- No evidence for such a signal → ULs
- Model: mixed background

$$\Omega_{\mathrm{GW}}(f;\Theta) = \sum_{(\mathrm{p})} \beta^{(\mathrm{p})}(f)\Omega^{(\mathrm{p})}_{\mathrm{ref}} F_{\alpha_{\mathrm{p}}}(f)$$

$$\beta^{(\mathrm{p})}(f) \equiv \gamma^{(\mathrm{p})}_{IJ}(f)/\gamma_{IJ}(f)$$

Current LVK results – constraints on non-GR pols

- Signal may include vector, scalar and tensor polarizations
- No evidence for such a signal → ULs
- Model: mixed background

$$\Omega_{\rm GW}(f;\Theta) = \sum_{\rm (p)} \beta^{\rm (p)}(f)\Omega^{\rm (p)}_{\rm ref} F_{\alpha_{\rm p}}(f)$$

$$\beta^{\rm (p)}(f) \equiv \gamma^{\rm (p)}_{IJ}(f)/\gamma_{IJ}(f)$$

- ULs at 95% CL:

Polarization	O1–O3	O1–O4a	Improvement
Tensor	$6.4 \cdot 10^{-9}$	$2.6 \cdot 10^{-9}$	~ 2.5
Vector	$7.9 \cdot 10^{-9}$	$2.9 \cdot 10^{-9}$	~ 2.7
Scalar	$2.1 \cdot 10^{-8}$	$7.4 \cdot 10^{-9}$	~ 2.8

- Signal versus noise Bayes factor:

$$\log_{10}\mathcal{B} = -0.87 \pm 0.01$$

- Non-GR vs GR Bayes factor:

$$\log_{10}\mathcal{B} = -0.44 \pm 0.03$$

LVK Collaboration, arXiv:2508.20721 (2025)

Current LVK results – magnetic budget

- Correlated magnetic noise:
  - Electronic mains
  - Synchronisation to GPS
  - Schumann resonances

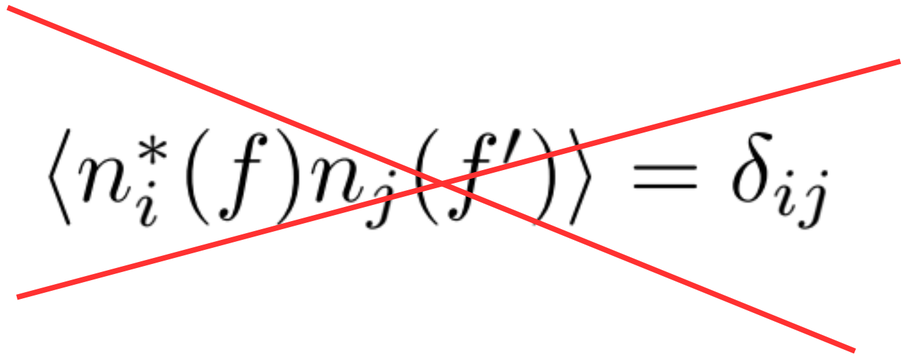

Current LVK results – magnetic budget

- Correlated magnetic noise:
  - Electronic mains
  - Synchronisation to GPS
  - Schumann resonances

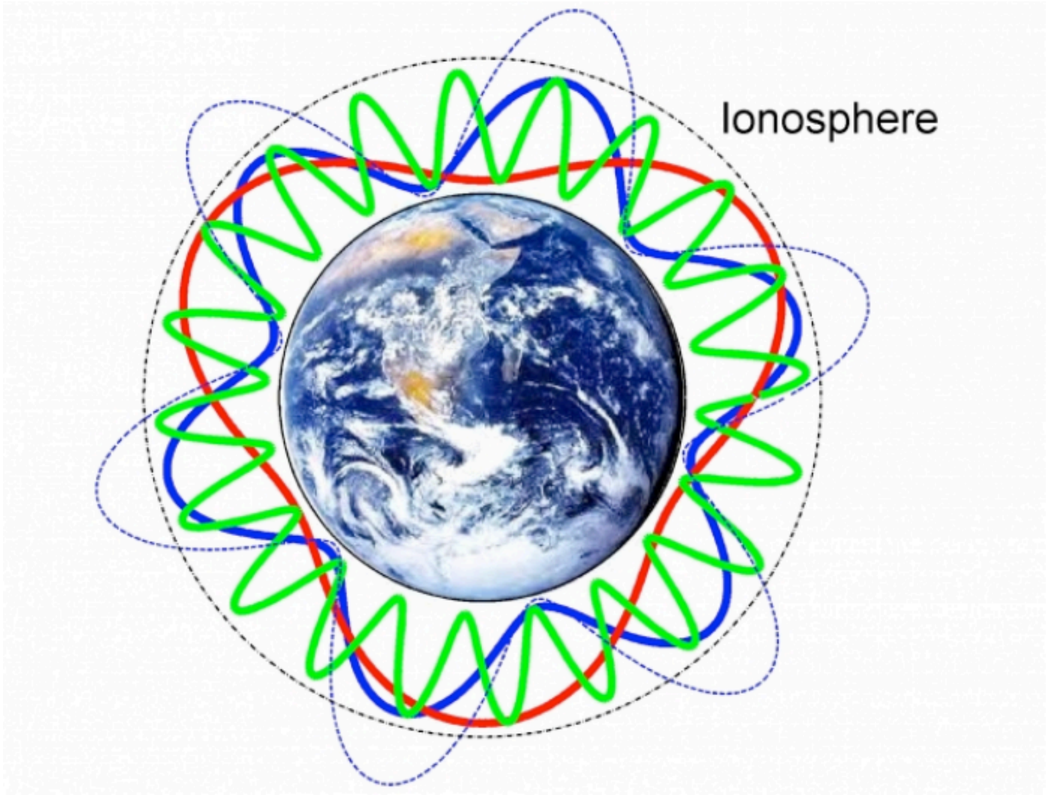

Current LVK results – magnetic budget

$$\hat{\Omega}_{\mathrm{mag},\,IJ}(f) = \frac{2}{T}\frac{|T_I(f)|\,|T_J(f)|\sqrt{\sum_{ab}|\tilde{m}^{\star}_{I,a}(f)\tilde{m}_{J,b}(f)|^2}}{\gamma_{IJ}(f)S_0(f)}$$

Current LVK results – magnetic budget

$$\hat{\Omega}_{\mathrm{mag},\,IJ}(f) = \frac{2}{T}\frac{|T_I(f)|\,|T_J(f)|\sqrt{\sum_{ab}|\tilde{m}^{\star}_{I,a}(f)\tilde{m}_{J,b}(f)|^2}}{\gamma_{IJ}(f)S_0(f)}$$

- ml,a(f): FTed magnetic data from the magnetic data of detector I

Current LVK results – magnetic budget

$$\hat{\Omega}_{\mathrm{mag},\,IJ}(f) = \frac{2}{T}\frac{|T_I(f)||T_J(f)|\sqrt{\sum_{ab}|\tilde{m}^{\star}_{I,a}(f)\tilde{m}_{J,b}(f)|^2}}{\gamma_{IJ}(f)S_0(f)}$$

- mI,a(f): FTed magnetic data from the magnetic data of detector I
- TI (f): magnetic coupling function of detector I

Current LVK results – magnetic budget

$$\hat{\Omega}_{\mathrm{mag},\,IJ}(f) = \frac{2}{T}\frac{|T_I(f)|\,|T_J(f)|\sqrt{\sum_{ab}|\tilde{m}^{\star}_{I,a}(f)\tilde{m}_{J,b}(f)|^2}}{\gamma_{IJ}(f)S_0(f)}$$

- mI,a(f): FTed magnetic data from the magnetic data of detector I
- TI (f): magnetic coupling function of detector I

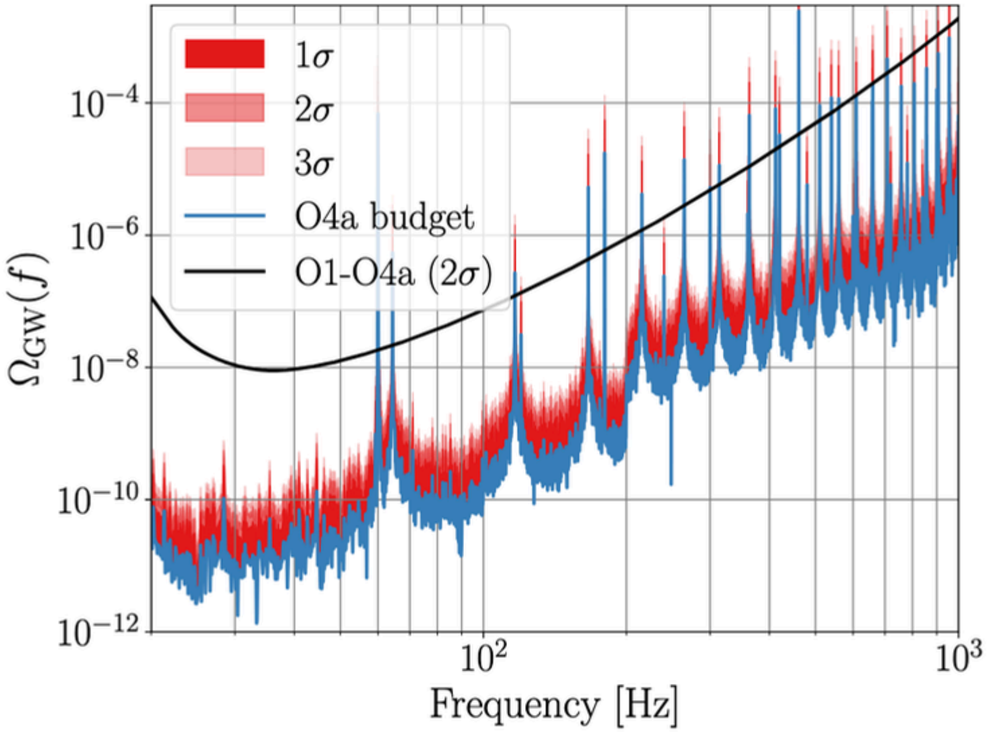

LVK Collaboration, arXiv:2508.20721 (2025)

LVK results – astrophysical implications

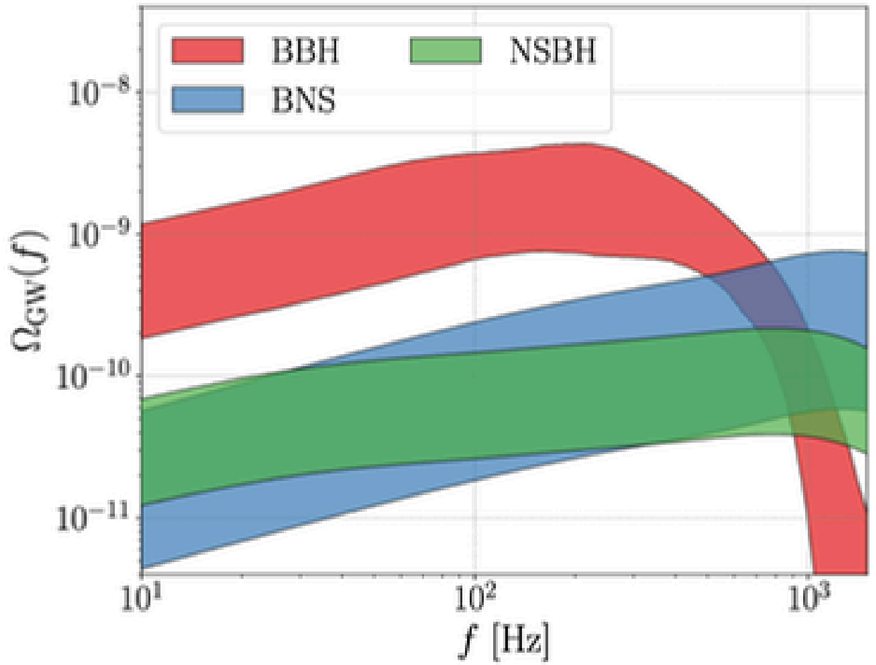

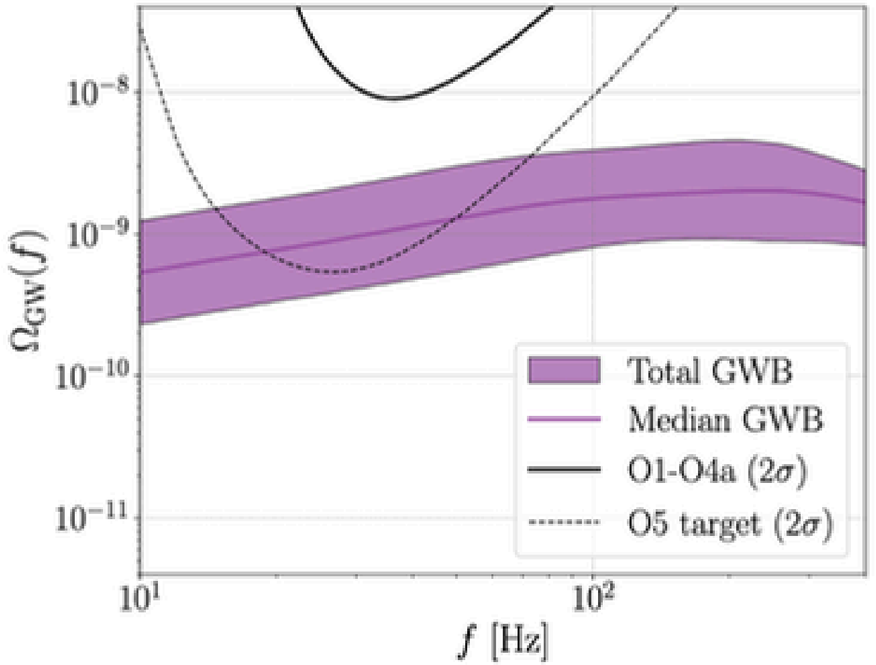

LVK Collaboration, arXiv:2508.20721 (2025)

LVK results – astrophysical implications

$$\Omega_{\mathrm{BBH+BNS+NSBH}}(25\mathrm{Hz}) = 0.9^{+1.1}_{-0.5} \times 10^{-9}$$

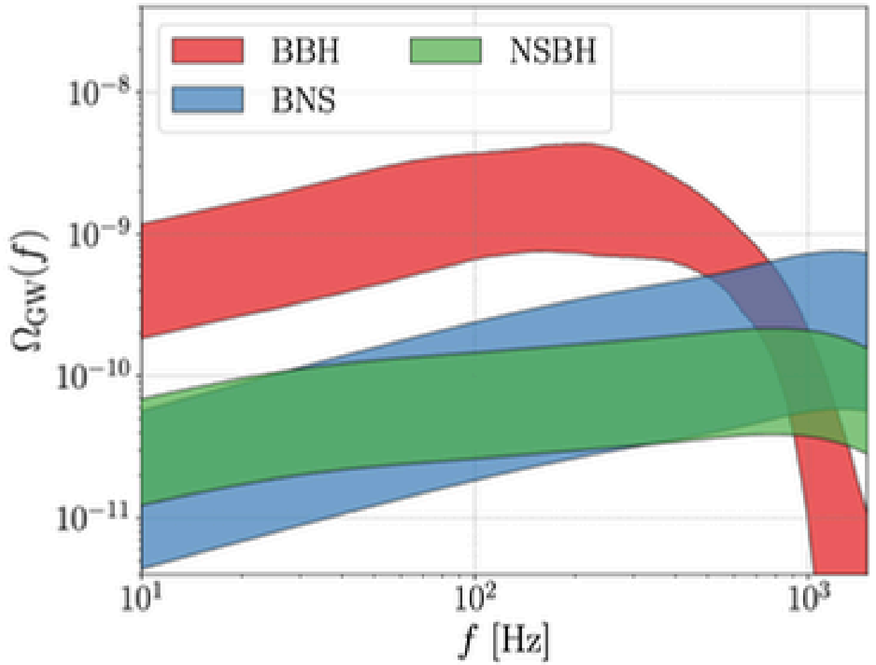

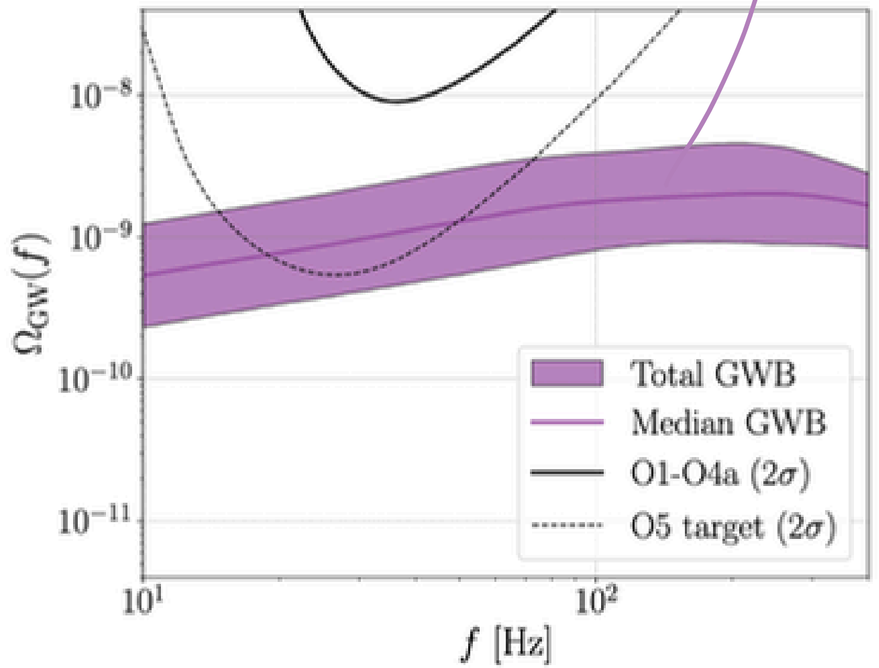

LVK Collaboration, arXiv:2508.20721 (2025)

LVK results – astrophysical implications

Detectable in A+?

$$\Omega_{\mathrm{BBH+BNS+NSBH}}(25\mathrm{Hz}) = 0.9^{+1.1}_{-0.5} \times 10^{-9}$$

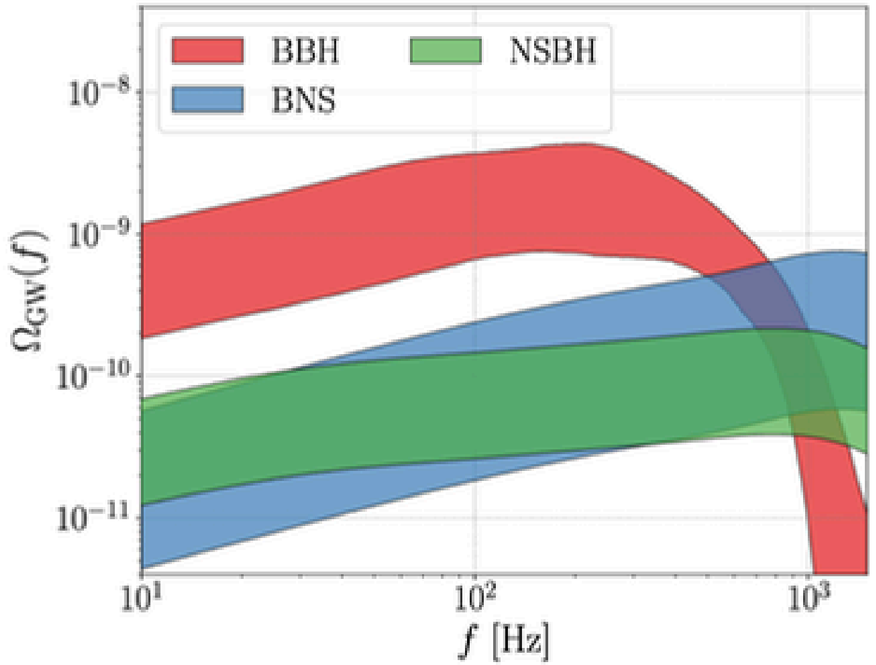

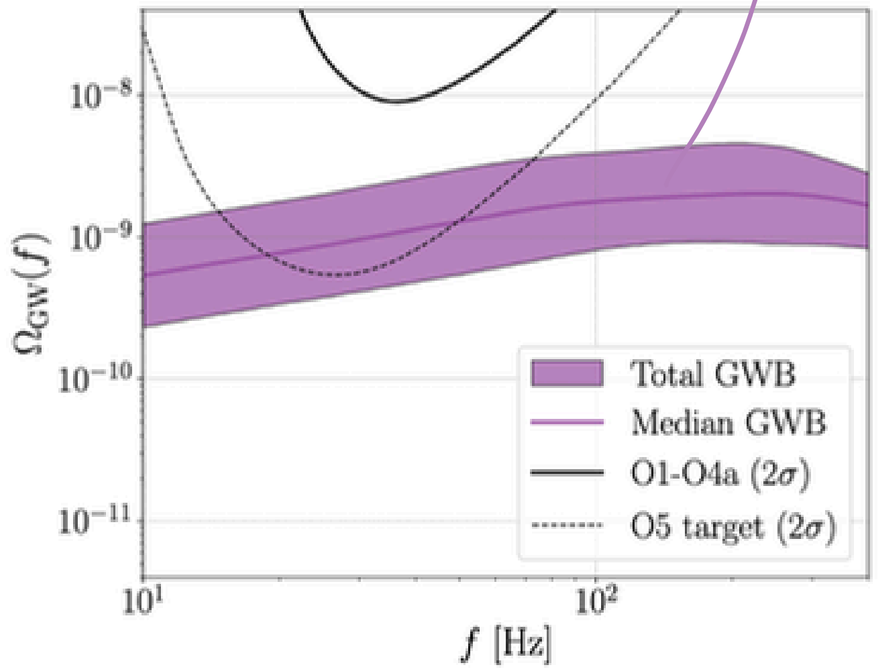

LVK Collaboration, arXiv:2508.20721 (2025)

Estimation of the CBC merger rate

Present-day merger rate is inferred to be:

- BBH: $15.4^{+6.0}_{-4.5}\,\mathrm{Gpc}^{-3}\,\mathrm{yr}^{-1}$
- BNS: $61^{+113}_{-48}\,\mathrm{Gpc}^{-3}\mathrm{yr}^{-1}$
- NSBH: $30^{+34}_{-19}\,\mathrm{Gpc}^{-3}\mathrm{yr}^{-1}$

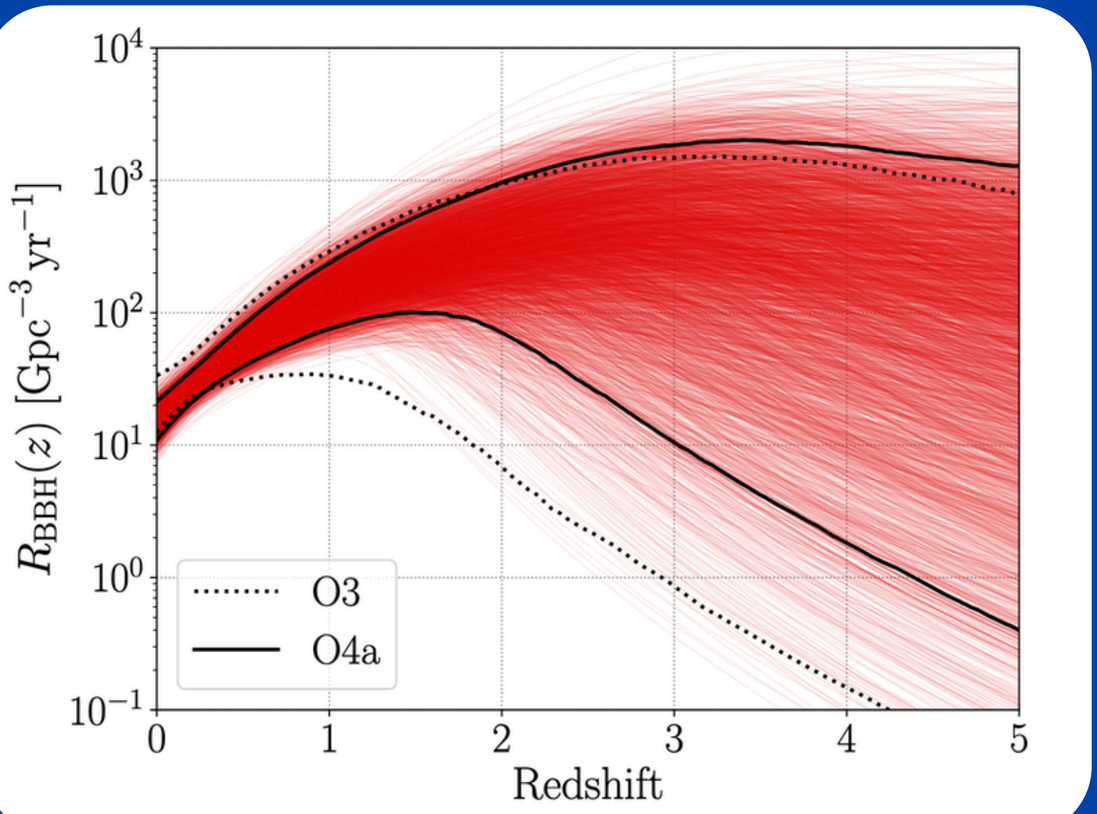

LVK Collaboration, arXiv:2508.20721 (2025)

Summary

- GWTC-4 and CBCpopulation properties:
  - 128 new CBC candidates (218 in total)
  - Some with SNR > 30
  - Mass distribution is the same as in O3 though better constrained
  - Merger rate evolution with z is consistent with star formation rate density
- Isotropic GWB search
  - No evidence for a signal → UL on the energy density: improvement ~ x2
  - No correlated magnetic noise
  - Possible detectable astrophysical foreground with A + sensitivity

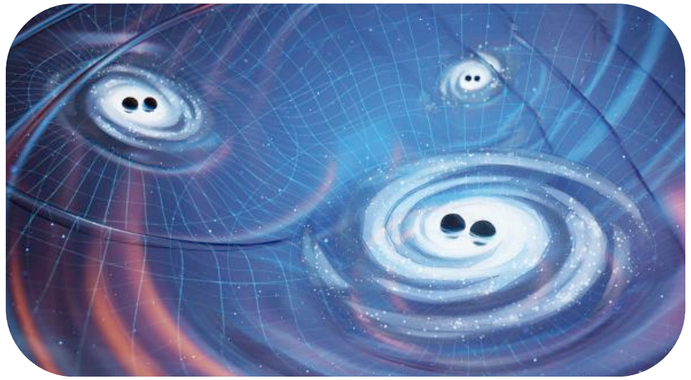

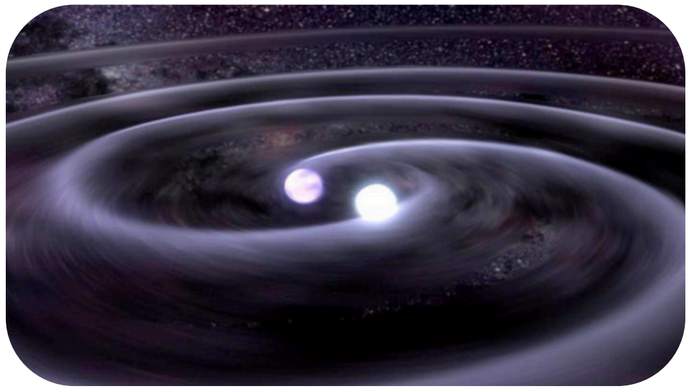

BACKUP

GW emission, quadrupole formalism

- Given a source at

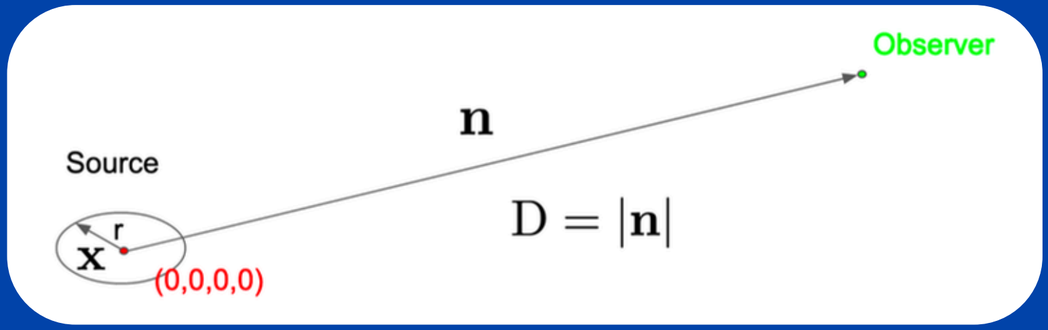

- A solution to E. eqs is given by

$$\bar{h}_{\mu\nu}(t,\mathbf{n}) = \frac{4}{D}\int d^3x T_{\mu\nu}(t-D,\mathbf{x})$$

GW emission, quadrupole formalism

- Given a source at

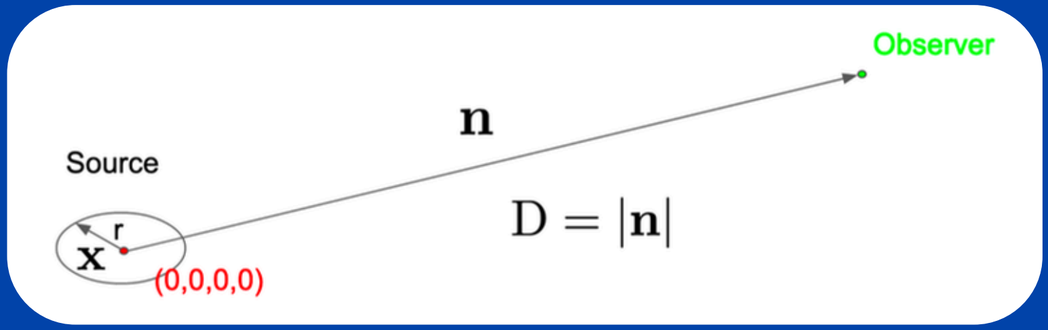

- A solution to E. eqs is given by

$$\bar{h}_{\mu\nu}(t,\mathbf{n}) = \frac{4}{D}\int d^3x T_{\mu\nu}(t-D,\mathbf{x})$$

amplitude of a GW decreases linearly with the distance

GW emission, quadrupole formalism

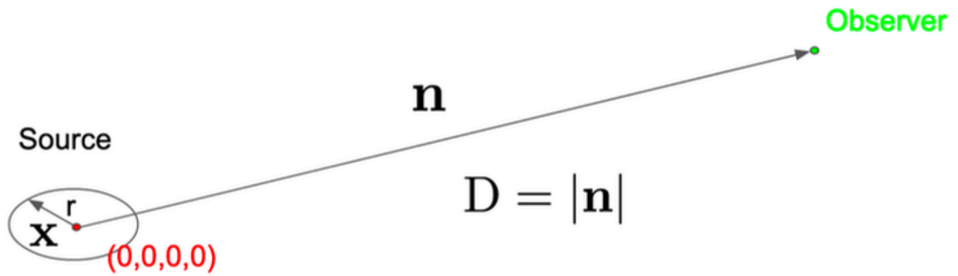

- Using the TT gauge the sol. can be further simplified:

$$h_{ij}^{TT}(t) = \frac{2}{D}\ddot{M}_{ij}(t - D)$$

GW emission, quadrupole formalism

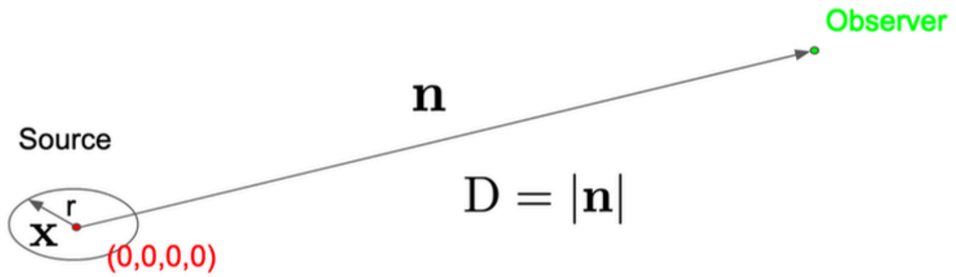

- Using the TT gauge the sol. can be further simplified:

$$h_{ij}^{TT}(t) = \frac{2}{D}\ddot{M}_{ij}(t - D)$$

$$M_{ij}(t) \equiv \rho(t, \mathbf{x})(x_i x_j - \frac{1}{3}r^2\delta_{ij})d^3x$$

mass quadrupole momentum

ρ(t,x): mass distribution of the source

GW emission, quadrupole formalism

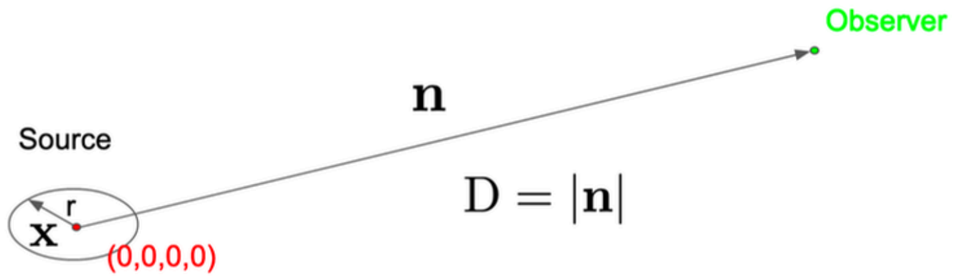

- Using the TT gauge the sol. can be further simplified:

$$h_{ij}^{TT}(t) = \frac{2}{D}\ddot{M}_{ij}(t - D)$$

Sources whose mass have a varying quadrupolar moment will generate time and amplitude dependent GW

LVK search for an isotropic GWB

Cross correlation spectrum (frequentist analysis)

$$\hat{C}^{IJ}(f) = \frac{2}{T}\frac{\mathrm{Re}[\tilde{s}_I^{\star}(f)\tilde{s}_J(f)]}{\gamma_{IJ}(f)S_0(f)}$$

$$\sigma^2_{IJ}(f) \approx \frac{1}{2T\Delta f}\frac{P_I(f)P_J(f)}{\gamma^2_{IJ}(f)S_0^2(f)}$$

$$S_0(f) = \frac{3H_0^2}{10\pi^2}\frac{1}{f^3}$$

Sensitivity of V1 for it to be useful for stochastic searches

	α=0	α=2/3	α=3
Same T_{obs}	1.00586425 (0.6%)	1.00862208 (0.9%)	1.05483612 (5.4%)
O4b only	1.00715552 (0.7%)	1.01046269 (1%)	1.0659603 (6.5%)
O4a+O4b	1.00337366 (0.3%)	1.00493719 (0.5%)	1.03156565 (3.2%)
Same T_{obs}, same PSDs	1.06825998 (6.8%)	1.09307502 (9.3%)	1.53873241 (54%)
$T_{obs,XV} = 2T_{obs,HL}$, same PSDs	1.13241281 (13%)	1.178824 (18%)	1.93271696 (93%)
$T_{obs,XV} = 2T_{obs,HL}$	1.01169451 (1.2%)	1.01717109 (1.7%)	1.10695912 (11%)
$T_{obs,XV} = 3T_{obs,HL}$	1.01749136 (1.7%)	1.02564883 (2.6%)	1.15673581 (16%)